6-1-1977

Dam Neck Current Analysis Dam Neck, Virginia Beach, Virgina

C. S. Welch
Virginia Institute of Marine Science

K. P. Kiley
Virginia Institute of Marine Science

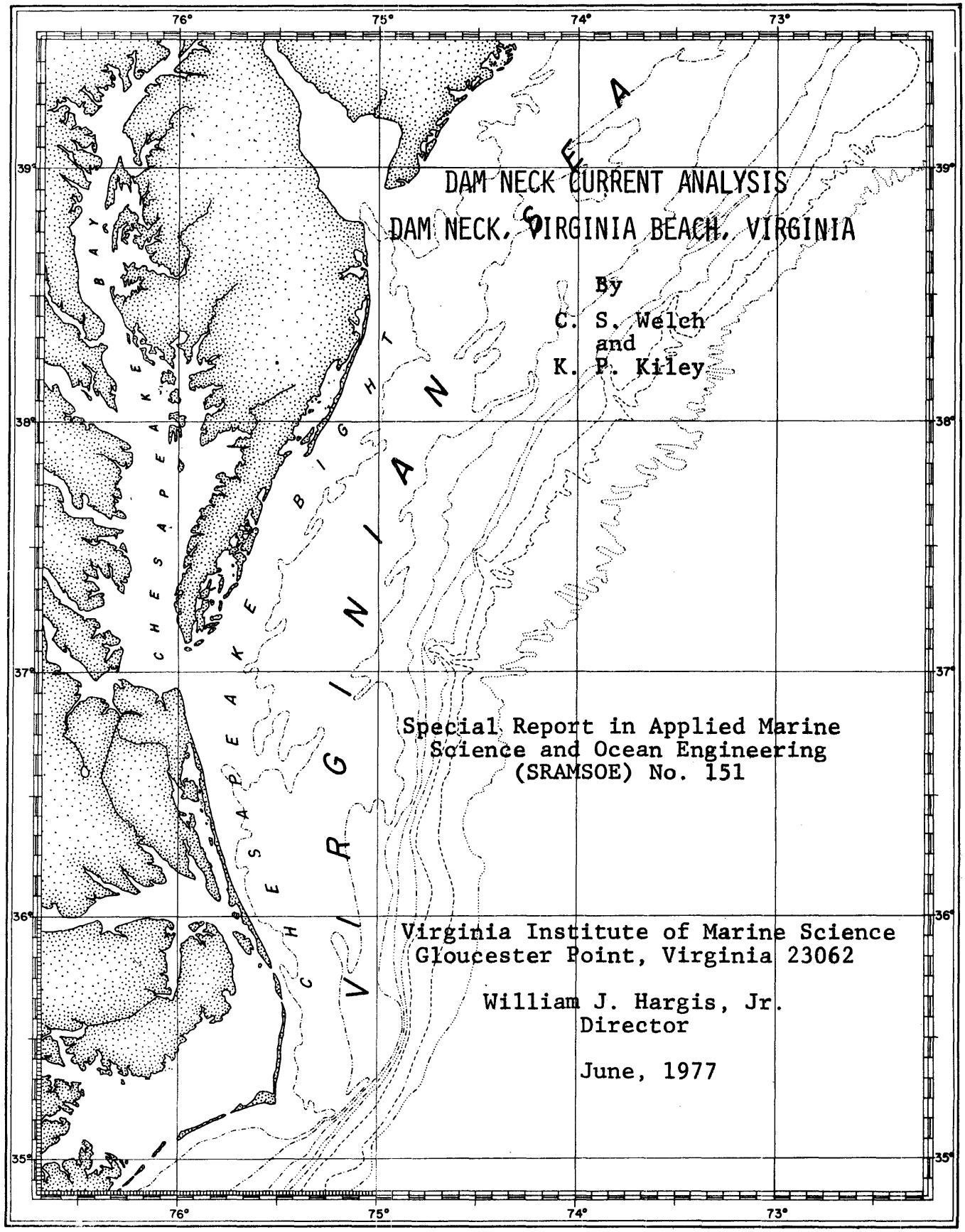

DAM NECK CURRENT ANALYSIS
DAM NECK, VIRGINIA BEACH, VIRGINIA

By

C. S. Welch
and
K. P. Kiley

Special Report in Applied Marine
Science and Ocean Engineering
(SRAMSOE) No. 151

Virginia Institute of Marine Science
Gloucester Point, Virginia 23062

William J. Hargis, Jr.
Director

June, 1977

DAM NECK CURRENT ANALYSIS

DAM NECK, VIRGINIA BEACH, VIRGINIA

by

C. S. Welch
and
K. P. Kiley

Special Report in Applied Marine
Science and Ocean Engineering
(SRAMSOE) No. 151

Virginia Institute of Marine Science
Gloucester Point, Virginia 23062

William J. Hargis, Jr.
Director

June, 1977

TABLE OF CONTENTS

LIST OF TABLES

LIST OF FIGURES

List of Figures (cont'd)

ACKNOWLEDGEMENTS

This work was made possible by a contract from Malcolm Pirnie Engineers, Inc. to examine currents from existing data near Dam Neck, Virginia. In particular, the assistance of Douglas Ensor and Dean Ramsay is appreciated. Elmer Richards, of Mueser, Rutledge, Wentworth and Johnston Consulting Engineers, also was most helpful.

We appreciate the assistance of John C. Ludwick of Old Dominion University in obtaining the missing current meter data for 4 Surf. I and for discussing the results of our research in this area.

The in-house work could not have been done so successfully without the continuing efforts of William Blystone, of the VIMS Computer Center. Shirley Crossley and Terry Markle were invaluable with their competent work in typing and drafting. The work could not have gone as smoothly as it did without the efforts of John Boon, III, who served well as project coordinator. The efforts of Robert J. Byrne were most important in initiating and reviewing the project.

ABSTRACT

Current records and meteorological records have been searched and interpreted to estimate some current related factors in the vicinity of Dam Neck, Virginia. The current data consists of approximately 30 day current meter records taken in summer 1973 and drogued buoy tracks recorded in autumn 1972. Estimated quantities include vector averaged current, maximum anticipated current associated with winter storms, tidal current ellipses, the seasons during which winter storms can be expected, and the keys to the end and beginning of the winter (stormy) season in any given year. A discussion of hurricanes is also included.

Dam Neck Current Analysis

1. Summary of Findings

1.1 Current records and meteorological records have been searched and interpreted to estimate some current related factors in the vicinity of the Atlantic Plant outfall site at Dam Neck, Virginia. (Figure 1.1). Estimated quantities include vector averaged current, maximum anticipated current associated with winter storms, tidal current ellipses, the seasons during which winter storms can be anticipated, and keys to the end and beginning of the winter (stormy) season in any given year. A discussion of hurricanes is also included.

1.2 The tidal currents at the Dam Neck site are oriented primarily parallel to the shoreline and are nearly bidirectional (ellipticity $\simeq$ 0.2). They have amplitudes between 15 (Neap tide) and 25 (Spring tide) cm/sec., or less than 1/2 knot. The regularity of the daily current as encountered in the rivers and bays locally is not found at this site. In local tidal rivers, up to 95% of the energy of water motion can be accounted for by the tides, but at the outfall site, approximately half the energy is related to tides. This means that the nontidal currents are typically as great as the tidal currents and although being generally coast parallel, they can be in any direction. Indeed, periods of several days duration are likely to be encountered at the outfall site

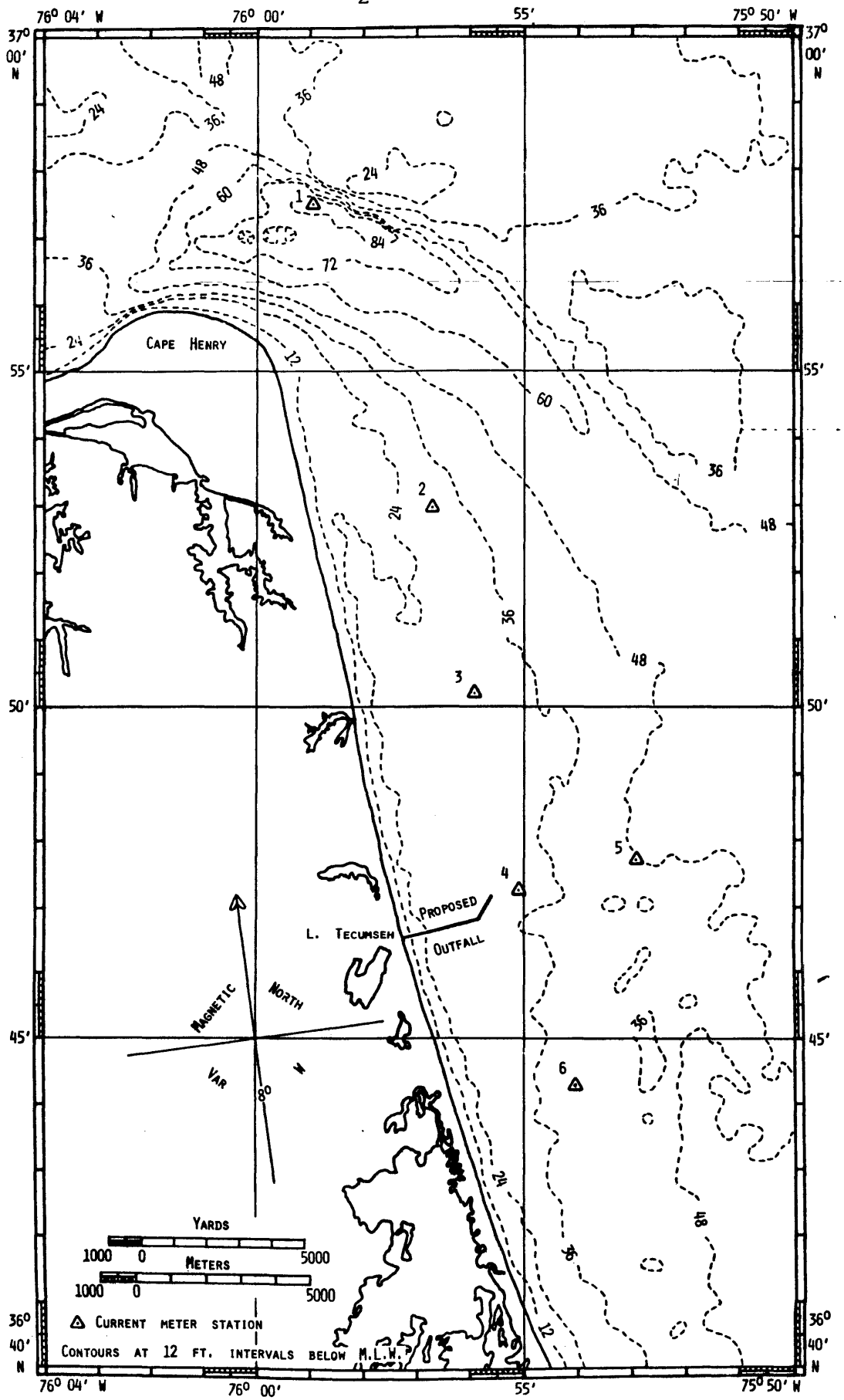

Figure 1.1. Location of proposed outfall at Dam Neck, Virginia. Current meter stations are included along with bathymetry (Goldsmith, Sutton and Sallenger, 1973 and Ludwick and Saumsiegle, 1976).

when the current remains essentially constant with little apparent tidal variation.

No time lag was detected in the tidal signal between any two of the current meters to a resolution of 90 minutes. An offset of about 100 minutes between the times of observed slack water at all analyzed stations and predicted slack water at Chesapeake Bay Mouth was found. As this offset remains unexplained, it prevents drawing a firm conclusion regarding the time correspondence between current and tidal height.

1.3 In the immediate site of interest, just seaward of the proposed outfall (station 4 bottom), the analyzed records indicate a vector averaged current so small near the bottom that it cannot from the data be distinguished from zero current. It is less than 1 cm/sec (.02 knots).

1.4 Winter storms can drive a general current southward along the entire continental shelf of the Mid-Atlantic Bight. The current meters recorded several such events during winter storms during the 1972-73 winter. The largest value of speed in these records was just under 2 knots. This value is comparable to the value of 1.3 knots reported by Beardsley (1974) further north in the Mid Atlantic Bight.

1.5 Winter storms are substantially more severe than any other normally encountered weather in the region of Dam Neck. Not only are wind speeds substantially greater than those encountered otherwise, but the winds come from an open ocean

direction with essentially unlimited fetch. These storms are limited to a particular period of the year. This period extends approximately from September 15 through April 15.

1.6 The key to the end of the winter storm season appears to be the establishment of the Bermuda High. This feature first occurs over the southeastern seacoast of the U. S. extending out to sea, and it becomes apparently dominant when its central pressures exceed 1028 millibars. The key to the beginning of the winter storm season appears to be the first establishment of the polar front passing south of Virginia. This front appears as a cold front "bulge" coming out of Canada and passes across Virginia in a southeastward direction.

1.7 The study region comes under the influence of hurricanes or tropical storms about .89 times each year. The frequency of hurricanes crossing the coast in a given year is much less, about .02. The effect of such a crossing on currents near an outfall is difficult to report, as few relevent measurements have been made. In one instance, a current meter outside the breaker zone on the Gulf Coast recorded speeds of 3.2 knots in pulses before it became inoperable due to damage from the storm.

2. Introduction

2.1 As part of the survey associated with the proposed Atlantic Plant Outfall site at Dam Neck, Virginia, this report consists of an analysis and discussion of currents to be expected near the site of the proposed outfall (Figure 1.1). The discussion addresses currents expected in the immediate vicinity of the outfall during its lifetime. The analysis has been applied only to data which are on hand; no new data have been taken as part of the study.

2.2 Estimates have been made of several quantities which may be related to the Atlantic Plant outfall site. Vector averaged current is the vector whose components consist of arithmetic means of the instantaneous current over a very long time period. It may be considered the mean value of the permanent current (Schureman, 1975). Tidal ellipses are estimated for the M_2 tide, the principal lunar semi-diurnal constituent (Schureman, 1975). This constituent has, by definition, perfectly sinusoidal components of velocity in time, so that the locus of the tip of the velocity vector forms a pure ellipse. As it is also the largest amplitude tidal constituent in the local area, the ellipse is a good indicator of the average tidal current cycle. During winter storm conditions, the currents driven by storms have speeds higher than those normally encountered. An estimate is made of the maximum expected speed during winter storms. As the name implies, winter storms occur

during a particular season of the year. An estimate of the limits of this season is made. Finally, the largest currents which may occur are those during hurricanes. A discussion of a single current meter record taken on the Gulf Coast during a hurricane is presented.

2.3 The astronomical tidal current can be well represented in this area by a sum of sinusoidal curves for each vector component. These curves oscillate in time with two families of frequency, one near twice per day (semidiurnal) and one near once per day (diurnal). The resultant tidal signatures vary from day to day as these various tidal harmonics tend to reinforce or cancel one another in the sum. The largest of these harmonics is called the principal lunar semidiurnal (M_2) tide. The current due to this single constituent must necessarily be in the form of an ellipse. We present charts showing the M_2 ellipse as observed at several positions along the coast in the study area. These charts exhibit several features which can be expected to apply to actual tides in the area. The shape of the ellipse should indicate the extent to which the observed current is either rotary or bi-directional. The size of the ellipse indicates the amplitude of the tidal current.

2.3.1 In general, the tidal current, so important in most port areas, diminishes with increasing distance seaward from the mouth of Chesapeake Bay. As part of our analysis, we compute the total amount of variance in the velocity

components (along and across the direction of the coast) which is accounted for in our tidal estimates. In many estuarine areas, this figure has amounted to 80-90% of the total variance. The ~50% we obtain in the study area indicates that tides are about as important as the non-tidal time-dependent currents, so the tidal prediction cannot reasonably be expected to be as central to current determination as in enclosed port areas.

2.4 Current speeds have been observed both in the study region and in similar situations in the mid-Atlantic Bight to be particularly large during winter "northeaster" storms. Data from several sources are combined in a discussion of the events, which are as yet not fully explained, with the object of producing an estimate of the currents from this phenomenon to be anticipated over the lifetime of the outfall.

2.5 Current speeds during a hurricane may well exceed those during a winter storm. As a guide to estimation of storm forces during a hurricane, we present the record (Murray, 1970) from a single current meter near the Gulf Coast during hurricane Camille, August 1969. The record is incomplete due to the destruction of the current sensors by the storm. The part which was taken indicates that the greatest currents which may occur in the region of interest may be associated with hurricanes. Also, we indicate records of pipeline movement in the Gulf of Mexico during hurricanes.

2.6 Because anomalously strong currents may be expected in the study region during winter storms, a discussion of the winter storm season is included. While the constructed outfall can be expected to encounter many winter storms during its life, the season for winter storms may be of interest in planning and executing the construction of the outfall.

3. Description of Data

3.1 Current Meter Data

3.1.1 Summary of Current Meter Data

3.1.1.1 Original Data - Top and bottom current meter data were recorded for 6 stations in the Virginia Beach/Dam Neck area during the July to October period in 1973. The data were collected by EG&G Environmental Engineering Services, Waltham, Massachusetts (Magas, 1973). EG&G reduced the data to 15 minute interval averages and transferred these averages to magnetic computer tape. VIMS received a copy of the computer tape and a computer listing of its contents from Malcolm Pirnie, Inc. The data for station 4 surface task I (4 Surf. I) were missing from this tape. A copy of these missing data was obtained from Old Dominion University and was subsequently transferred and converted to the VIMS edited current meter tape. A detailed description of the current meter data processing is given in appendix 2.

3.1.1.2 Data Conversion

The current meter data were converted to the VIMS current meter data format. As part of the conversion process, complete header labels were appended to each current meter file. Two computer tapes were produced: a current meter data tape and an edited current meter data tape, (the data base for the tidal analysis program).

3.1.2 Original Data

Current meter data was collected at 6 stations in the Virginia Beach/Dam Neck Area (Figure 1.1). Current meters were deployed during three separate sampling periods, each lasting about a month, as shown in Table 3.1. Each station consisted of two current meters, a subsurface float, and an anchor. The current meters were Geodyne type 102 film recording current meters. These meters use a Savonius rotor to sense current speed and a vane within a cage to sense current direction, in conjunction with an internal compass. The current meters were sampled at 5 minute intervals. EG&G reduced these data to 15 minute vector average readings and transferred the averaged readings to magnetic computer tape. A summary of these data is given in Table 3.2. Each reading consists of a speed and direction for the averaged current.

Table 3.1. Current Meter Deployment Periods

Period	Starting Date	Stations Sampled
Task I	7/21/73	1,2,3,4,5,6
Task II	9/2/73	4
Task III	9/30/73	1,3,4,5,6

3.1.3 Data Conversion

3.1.3.1 The current meter data was converted to the VIMS current meter data format in order to be compatible with our analysis software. As part of the conversion, header labels were appended to each current meter file. Included

Table 3.2. Dam Neck Current Meter Data Received by VIMS

Task	Station	Depth	VIMS Tape File No.	Current Meter Record No.	Record Date	Start Time	No. of Readings	Speed Factor
I	1	Surface	2	403105	7/22	1515	2650	1.25
I	1	Bottom	3	403102	7/21	0715	2777	1.25
I	2	Surface	4	403101	7/22	1755	2664	1.25
I	2	Bottom	5	403100	7/21	1217	474	1.25
I	3	Surface	6	403104	7/21	1150	2780	1.25
I	3	Bottom	7	403108	7/21	1150	2781	1.25
I	4	Surface	24	403111	7/21	1030	3321	1.25
I	4	Bottom	1	403110	7/21	1030	3282	1.25
I	5	Surface	8	403106	7/21	1055	2777	1.25
I	5	Bottom	18	403107	7/21	1100	2782	1.00
I	6	Surface	19	403109	7/21	0940	2777	1.00
I	6	Surface	20	403103	7/21	0935	1010	1.00
I	*	"	21	403103	7/21	*	8359	*
II	4	Surface	22	403112	9/2	0725	2714	1.00
II	4	Bottom	23	403113	9/2	0725	2714	1.00
III	1	Surface	9	403122	9/30	1109	360	1.25
III	3	Surface	14	403120	9/30	1215	2982	1.25
III	3	Bottom	15	403121	9/30	1215	2949	1.25
III	4	Surface	10	403118	9/30	1330	2966	1.25
III	4	Bottom	11	403119	9/30	1330	2970	1.25
III	5	Surface	12	403116	9/30	1500	2959	1.25
III	5	Bottom	13	403117	9/30	1500	2931	1.25
III	6	Surface	16	403115	9/30	1400	2966	1.25
III	6	Bottom	17	403114	9/30	1400	2966	1.25

* not given

in these header files are position and depth of the current meter. Latitude and longitude were obtained from a chart of the deployment positions (Magas, 1973). Depths of the current meters were obtained from EG&G. (personal communication). These depths, expressed in feet above the sea floor, were converted to feet below mean low water. Values of latitude, longitude and depth for each record are given in Table 3.3. In addition to the header labels, the VIMS data carry an explicit time value for each reading. The starting time and time increment were supplied to the conversion program, which generated the required value.

3.1.4 Tidal Current Data

3.1.4.1 Predicted slack water times at Chesapeake Bay Entrance (NOS, 1972) were used for calculating time differences between slack water at Chesapeake Bay Entrance and the current meter stations.

3.2 Buoy Data Description

3.2.1 The buoy data used in the analysis come from the joint VIMS-NASA Langley Research Center (LaRC) project to use the capability of the French EOLE satellite. The project (Ruzecki, et al., 1976) involved the release of several sets of drogued buoys (described by Wallace and Cox, 1976). Two of the experiments are of particular interest for this report, because buoys drifted into and through the study area (data reported in Usry and Wallace, 1975) and Wallace and Usry, 1976). These instances occurred during December 1972 and February 1973. In the December drift, (Ruzecki, et al., 1976) the data were compared with a purely wind driven theory.

Table 3.3. Current Meter Latitude, Longitude, and Depth.

Task	Station	Latitude(N)	Longitude(W)	Location	Depth (ft.)
I	1	36°57'33"	75°58'56"	Surface	29
I	1	"	"	Bottom	72
I	2	36°53'01"	75°56'41"	Surface	15
I	2	"	"	Bottom	21
I	3	36°50'13"	75°55'53"	Surface	14
I	3	"	"	Bottom	24
I	4	36°47'14"	75°55'02"	Surface	14
I	4	"	"	Bottom	26
I	5	36°47'42"	75°52'50"	Surface	14
I	5	"	"	Bottom	44
I	6	36°44'14"	75°53'59"	Surface	14
I	6	"	"	Bottom	26
II	4	36°47'14"	75°55'53"	Surface	14
II	4	"	"	Bottom	26
III	1	36°57'33"	75°58'56"	Surface	25
III	3	36°50'13"	75°55'53"	Surface	16
III	3	"	"	Bottom	24
III	4	36°47'14"	75°55'02"	Surface	15
III	4	"	"	Bottom	26
III	5	36°47'42"	75°52'50"	Surface	16
III	5	"	"	Bottom	44
III	6	36°44'14"	75°53'59"	Surface	16
III	6	"	"	Bottom	35

4. Methods of Data Analysis

4.1 Current Meter Data Analysis

4.1.1 The current meter data were analyzed using a method developed at VIMS for the analysis of short current meter records (as short as 3 days)(Lewis, 1975). It is based on the work of Munk and Cartwright (1966) as cited in Wunsch (1972).

4.1.2 The VIMS routine, named the TIPORAL program for TIdal POtential RAtio Lag, is designed to estimate the amplitude of the major tidal constituents from records too short to achieve frequency resolution in the spectra of the major semi-diurnal constituents, in particular the M_2 and N_2 constituents, which have a frequency difference of about 1/29 cycles per day.

4.1.3 The TIPORAL analysis, following Munk and Cartwright, first generates a partial gravitational tidal potential curve at the location of the current meter, the partial curve being the sum of the five greatest tidal constituents in the mid-latitudes, two diurnal (K_1, O_1) and three semi-diurnal (M_2, S_2, N_2). This curve is generated for the period of the record to be analyzed truncated to the greatest integral number of lunar days (24.84 hours) within the record. The vector components of the observed current with orientation estimated to be that of the tidal current are also calculated. Each of these curves can be represented as a Fourier series in the following form

$$f(t) = \bar{f} + \mathrm{Re} \sum_{n=1}^{N/2} A_n \exp (i\, 2\pi n/T)$$

where A_n is a complex amplitude, N is the total number of values in the truncated series, T is the length of the truncated series, and i is the imaginary unit. The A_n's for this representation are calculated for n=1, 72 for each vector component and the tidal potential curve. The ratio of the complex amplitude of each vector component to that of the complex amplitude of the tidal potential at the corresponding n is called the response function for the component. The response function is calculated for each component for values of n from 1-72 for each series. To this point, the analysis technique is standard. Additional steps were designed to handle the short nature of the time series for which the technique was designed.

4.1.4 Because the tidal constituents of short time series are not resolvable, the assumption is made that the same response function value (both magnitude and phase) applies to all the constituents within a group (diurnal or semidiurnal). These two values are used as multipliers of the corresponding constituents of the tidal potential function to produce a calculated tidal current for each vector component. The calculated tidal current is subtracted from the original to produce a residual current component, and the reduction of variance is calculated as a figure of merit. For short records in particular, variance contributions due to the semidiurnal peak can "spill over" to affect the complex amplitude in the diurnal frequency band, producing a corresponding change in the response function. To alleviate this problem to some extent, the TIPORAL program

permits "manipulation" of the multipliers. Manipulation consists of an alteration of the values and a recalculation of the residual current and the reduction of variance. The multiplier values which produce the greatest reduction of variance are chosen as the ones most representative of the tidal currents at the position of the current meter.

4.1.5 The TIPORAL program also contains a provision for the calculation of overtides in order to remove as much periodic fluctuation as possible from the residual record. This feature was not used in the present analysis because the highest calculated frequency (72/29 CPD) is lower than the lowest frequency associated with overtides. Experimental runs of short segments from the 29 day records indicated a detectable variance in the overtides.

4.2 Current Meter Tidal Ellipses

4.2.1 The tidal ellipse we have calculated is the pure ellipse corresponding to the observed current at the frequency of the principal lunar semi-diurnal (M_2) constituent. As the M_2 constituent has the largest amplitude in the local tidal current, its ellipse is a good estimator of the local tidal current. Also, the difference between the M_2 current ellipses at various stations are good indicators of differences in the semi-diurnal tidal current response.

4.2.2 The current ellipses are constructed from the data produced by the TIPORAL program using the following conventions.

If an ellipse is parametrically defined by two sinusoidal components, time being the parameter,

$$y = B \cos(\omega t + \beta)$$

$$x = A \cos(\omega t + \alpha)$$

where y and x correspond to our longitudinal and lateral current components, α and β correspond to phase angles with respect to a tidal potential component, t is time, ω is the radian frequency of the M_2 tide, and A, B are the amplitudes of the lateral and longitudinal components respectively. The actual tidal ellipse is rotated by an angle (θ) to the orthogonal axes, θ being given by

$$\theta = \frac{1}{2} \tan^{-1} \frac{2AB\cos(\alpha-\beta)}{A^2 - B^2}$$

The major and minor axes of the ellipse have lengths

$$A_{Major} = 2 \frac{AB|\sin(\alpha-\beta)|}{\{P^2 - |F|\}^{1/2}}$$

$$A_{Minor} = 2 \frac{AB|\sin(\alpha-\beta)|}{\{P^2 + |F|\}^{1/2}}$$

Where $P^2 = \frac{A^2 + B^2}{2}$

and $F = \frac{B^2 - A^2}{2 \cos 2\theta}$

The ellipticity can be defined as

$$\varepsilon = \frac{A_{Minor}}{A_{Major}} = \left(\frac{P^2 - |F|}{P^2 + |F|}\right)^{1/2}$$

ε varies between 0 (for a reversing tide) and 1 (for a circular

rotating tide) and indicates the extent to which a given tidal ellipse can be considered rotary or purely reversing.

The sense of rotation is

counterclockwise (ccw) if $180^{o} < \beta-\alpha < 360^{o}$

clockwise (cw) if $0 < \beta-\alpha < 180^{o}$.

The time difference between the maximum current speed on the ellipse and that of the longitudinal component is given by

$$\Delta t = \frac{1}{\omega} \left(\beta - \tan^{-1}\left(\frac{B\sin\beta - A\tan\theta\sin\alpha}{B\cos\beta - A\tan\theta\cos\alpha}\right)\right)$$

These formulas were used to generate a tidal ellipse for each current meter for which the TIPORAL analysis was done.

4.2.3 Slack water time differences were calculated between each current meter record and the predicted time of slack water at Chesapeake Bay Entrance.

The following method was used. The orientation of the orthogonal axes was chosen so that the longitudinal axis would be roughly parallel to the coastline. We anticipated that the longitudinal axis would account for much of the tidal current. The small values of θ, the angle of rotation required to obtain the principal axes of the tidal ellipse from the longitudinal and lateral components, demonstrate that the longitudinal axis is a good estimate of the major axis of the tidal ellipse. (see Table 5.2).

From the TIPORAL plot of current meter readings for the longitudinal axis, observed slack water was chosen as the time when the general trend of the current readings crossed zero.

4.3 Analysis of drifting buoy data

The data from the drift buoys consist primarily of a series of measurements of positions of the buoy by the EOLE satellite whenever the satellite passed over the buoy. In addition, as part of the interrogation/reply sequence, the buoy sends its identification and several values of data of various kinds. For our experiments, the auxiliary data were usually temperature measurements. Each burst of data was reduced to a single estimate of position, time, and telemetered data. These estimates are the raw data received by VIMS. The analysis has consisted of plotting the position data in component form and generating an hypothesized position history from wind data from various nearby shore and light stations. As will be shown in the discussion section (5.6), this analysis has raised enough questions that more delicate analyses have not been undertaken.

5. Discussion of Results

5.1 Nearshore Current Regimes

Associated with a shoreline having a beach, there are several boundary regions in which currents of a purely local nature can be generated. The primary current systems in these local regions are the longshore drifts associated with surface waves impinging on the beach and rip currents. Beyond this nearshore region, currents are related to circulation on a broader scale. It is the currents outside the zone of wave-induced current systems with which the analyses in this report are concerned.

5.2 Vector Averaged Currents

The vector averaged current values calculated from the data are shown on Figure 5.1 for a coincident set of data (task I, July 21-August 19, 1973). Two points of note may be obtained from these values. First, the mean current speed at the mouth of Chesapeake Bay (station 1) is quite large (~0.2 kt.) and landward (up bay) at both meters. The mean current here is plausibly due to the estuarine circulation cell, and is expected to be out of the bay at the surface. The observed value indicates that the nominal surface current meter, at a depth of 29 ft., is actually in the lower part of the estuarine circulation cell. It is possible, then, that it does not represent the current at the surface well and that this difference accounts for the time offset between the observed and predicted slack water. (Fig. 5.4). The second point of note is that stations

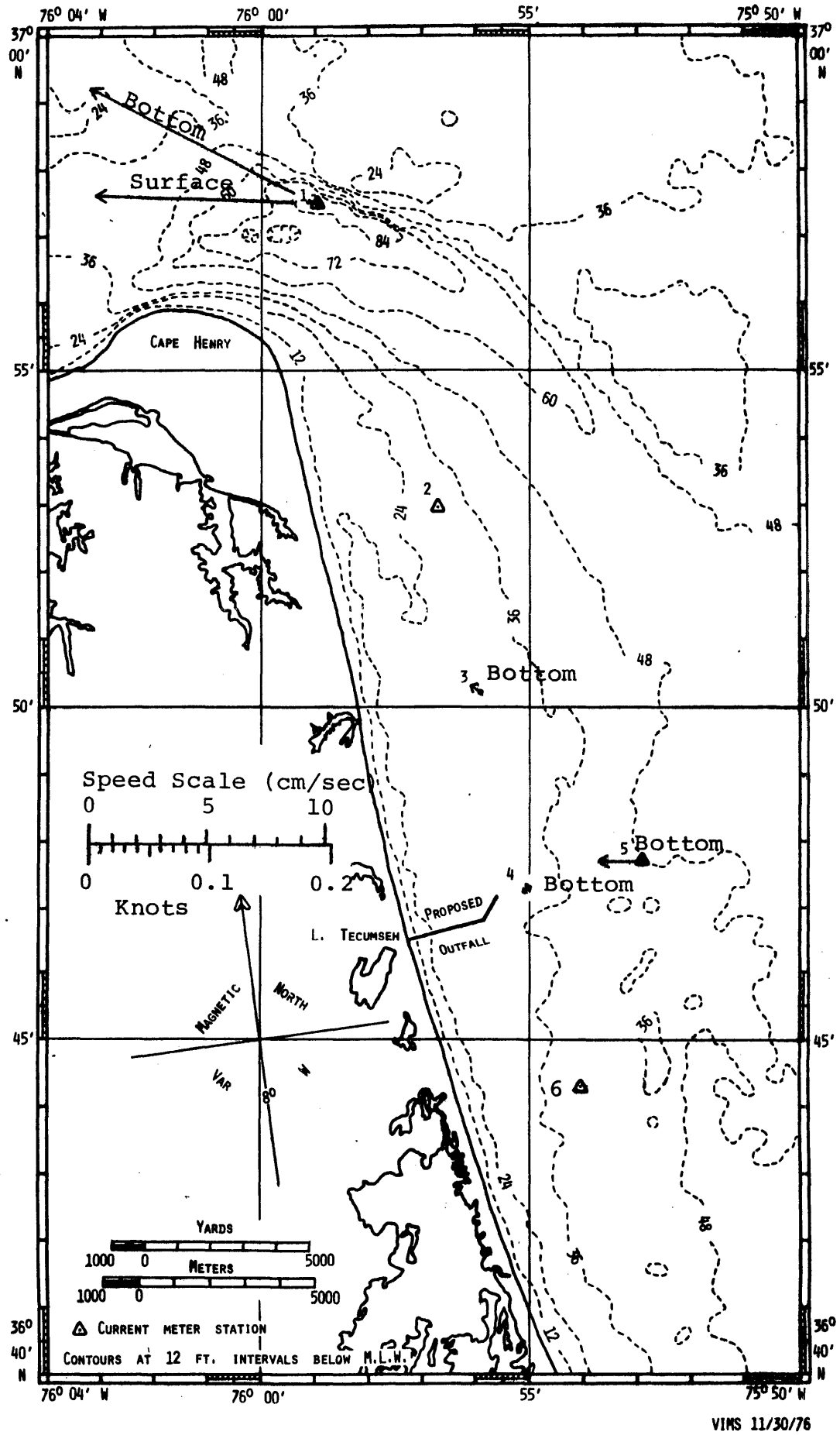

Figure 5.1. Mean velocities calculated for task I data. (21 VII 73 - 19 VIII 73).

3 and 4 both show nearly zero vector averaged current at the bottom. This implies that there is a region of at least several miles extent in the longshore direction in which little mean current due to tidal rectification occurs.

5.2.1 The mean current values from the later deployment (Task III, 30 IX 73 - 29 X 73) are not so consistent in their interpretation. The period of time during which task III was performed included several meteorological frontal passages as well as a tropical storm passing offshore. These produced a non-tidal fluctuating current which is indicated by low frequency variance in the record. In addition, some records show substantial wave contamination or similar effects. In the presence of these phenomena, it is doubtful whether mean values obtained during task III are particularly representative of the area in general. Table 5.1 lists the average current components at station 4, surface and bottom, and 6 bottom for task III. Taken by itself, station 4 presents the plausible situation

Table 5.1

Mean Currents in Study Area for Task III

Station	Depth	Along Shore (Towards 347°T)	Offshore
4	Surface	-5.7 cm/sec.	+ 1.3 cm/sec.
4	Bottom	-3.1 cm/sec.	- 1.3 cm/sec.
6	Bottom	+0.8 cm/sec.	- 0.2 cm/sec.

of a modest southward current having a profile decreasing with depth and a surface offshore component balanced by a deeper

onshore component. This situation is not corroborated at station 6, which shows a small current directed opposite to that at station 4.

5.3 Tidal Currents

Tidal ellipse calculations were performed for records 1 Surf. I (Station 1, Surface meter, task I), 1 Bot. I, 3 Bot. I, 4 Surf. I, 4 Bot. I, 4 Surf. III, 5 Bot. I, and 6 Bot. III. The velocity component amplitudes and phases are listed in table 5.2, while the ellipse parameters derived from these using the formulas listed in section 4.2.2 are shown in table 5.3 . The tidal ellipses for the principal semi-diurnal tidal current (M_2) are shown for selected stations in figure 5.2a for the surface and 5.2b for the bottom. Each ellipse is characterized by its major and minor axes and an arrow denoting sense of rotation. In the study region, the bottom tidal current is nearly reversing, as values of ellipticity are everywhere less than 0.2. The current is oriented nearly parallel to shore with an amplitude of 10-20 cm/sec. (0.2 - 0.4 kt.). Near the outfall site, the tidal currents are reduced from north to south. The slight apparent decrease in the offshore direction may not be significant. The tidal currents near the proposed outfall, in summary, appear to be on the fringe of the region affected principally by Chesapeake Bay tidal flow.

5.4 An examination of the current meter records indicates several periods of time when the current does not reverse with tidal periodicity as the tide is overcome by a long term

Table 5.2

Tidal Ellipse Variables

Station/ Task	A (Latr.Axis cm./sec.)	α (deg.)	B (Long.Axis cm./sec.)	β (deg.)	ω (deg/hr)
1 Surf. I	5.99	247.57	50.67	217.59	28.98
1 Bot. I	1.30	23.09	29.32	224.07	28.98
3 Bot. I	4.485	173.46	16.613	221.85	28.98
4 Surf. I	4.94	192.42	15.59	82.98	28.98
4 Bot. I	2.11	113.63	10.82	224.44	28.98
4 Surf. III	3.165	-6.40	15.499	92.57	28.98
5 Bot. I	1.66	223.95	8.62	238.70	28.98
6 Bot. III	1.030	33.71	6.267	217.41	28.98

Table 5.3. Tidal Ellipse Parameters

Station/ Task	Orientation (°T)	θ	Major Axis (cm./sec.)	(knots)	Minor Axis (cm./sec.)	(knots)	ε
1 Surf. I	293°	-5.87°	101.79	(1.98)	5.97	(0.12)	0.059
1 Bot. I	295°	2.37°	58.19	(1.13)	0.93	(0.02)	0.016
3 Bot. I	1°	-10.57°	33.78	(0.66)	6.60	(0.13)	0.195
4 Surf. I	340°	6.60°	31.37	(0.61)	9.26	(0.18)	0.295
4 Bot. I	343°	4.10°	21.70	(0.42)	3.94	(0.08)	0.181
4 Surf. III	345°	1.90°	31.00	(0.60)	6.25	(0.12)	0.202
5 Bot. I	358°	-10.57°	17.67	(0.34)	0.83	(0.02)	0.047
6 Surf. III	337°	9.32°	13.17	(0.26)	0.13	(.00)	0.010

Station/ Task	ΔT (min.)	Rotation	Slack Water Time Difference Ave. Diff. (min.)	Std. Dev. (min.)
1 Surf. I	-0.7	ccw.	106.5	80.0
1 Bot. I	0.1	ccw.	120.9	85.8
3 Bot. I	4.3	cw.	104.9	62.7
4 Surf. I	-4.1	cw.	62.1	78.9
4 Bot. I	-1.5	cw.	111.0	76.4
4 Surf. III	-0.8	cw.	58.4	79.8
5 Bot. I	1.1	cw.	148.8	64.5
6 Surf. III	0.2	ccw.	90.4	105.9

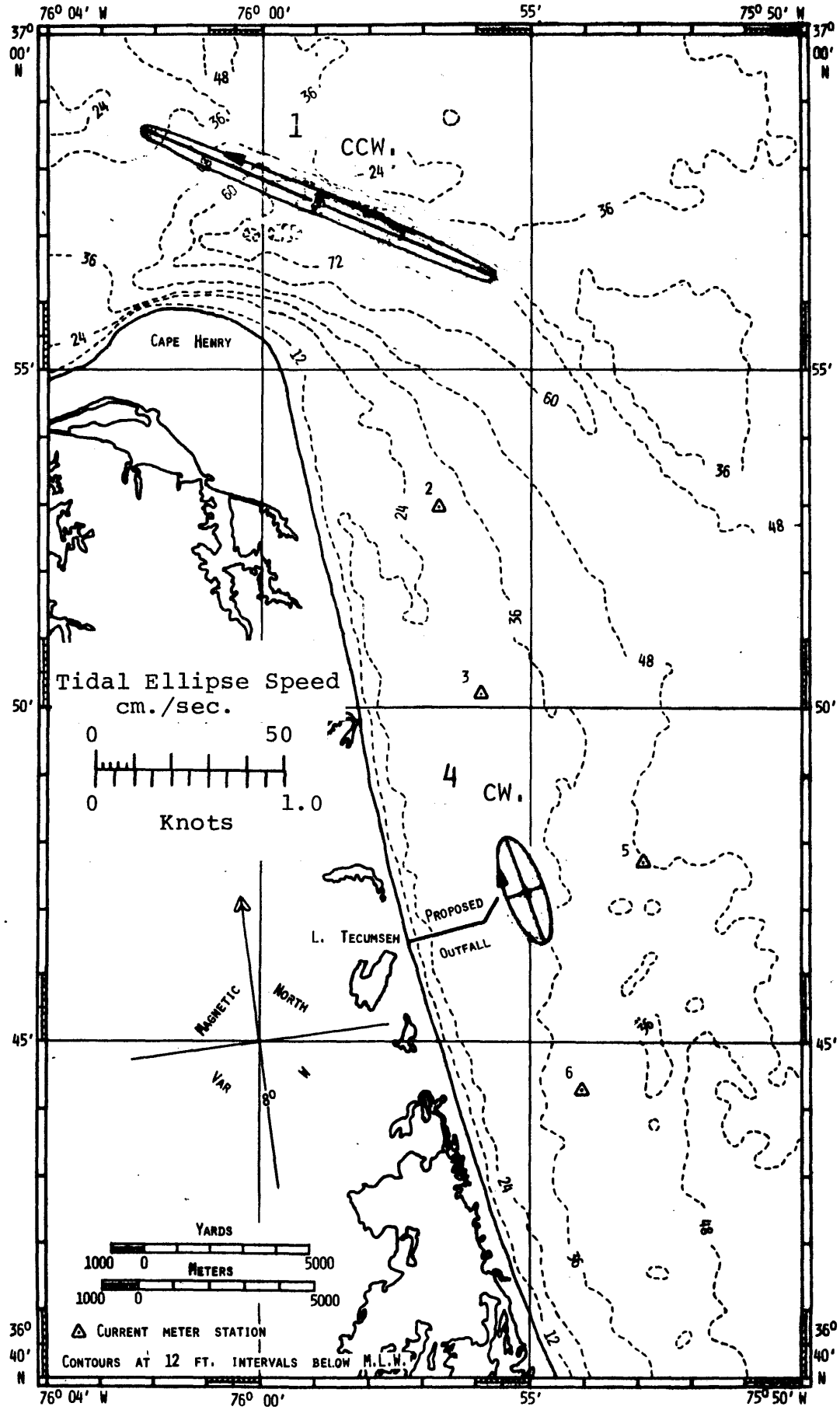

Figure 5.2a. Surface current meter station M_2 tidal ellipses for Task I.

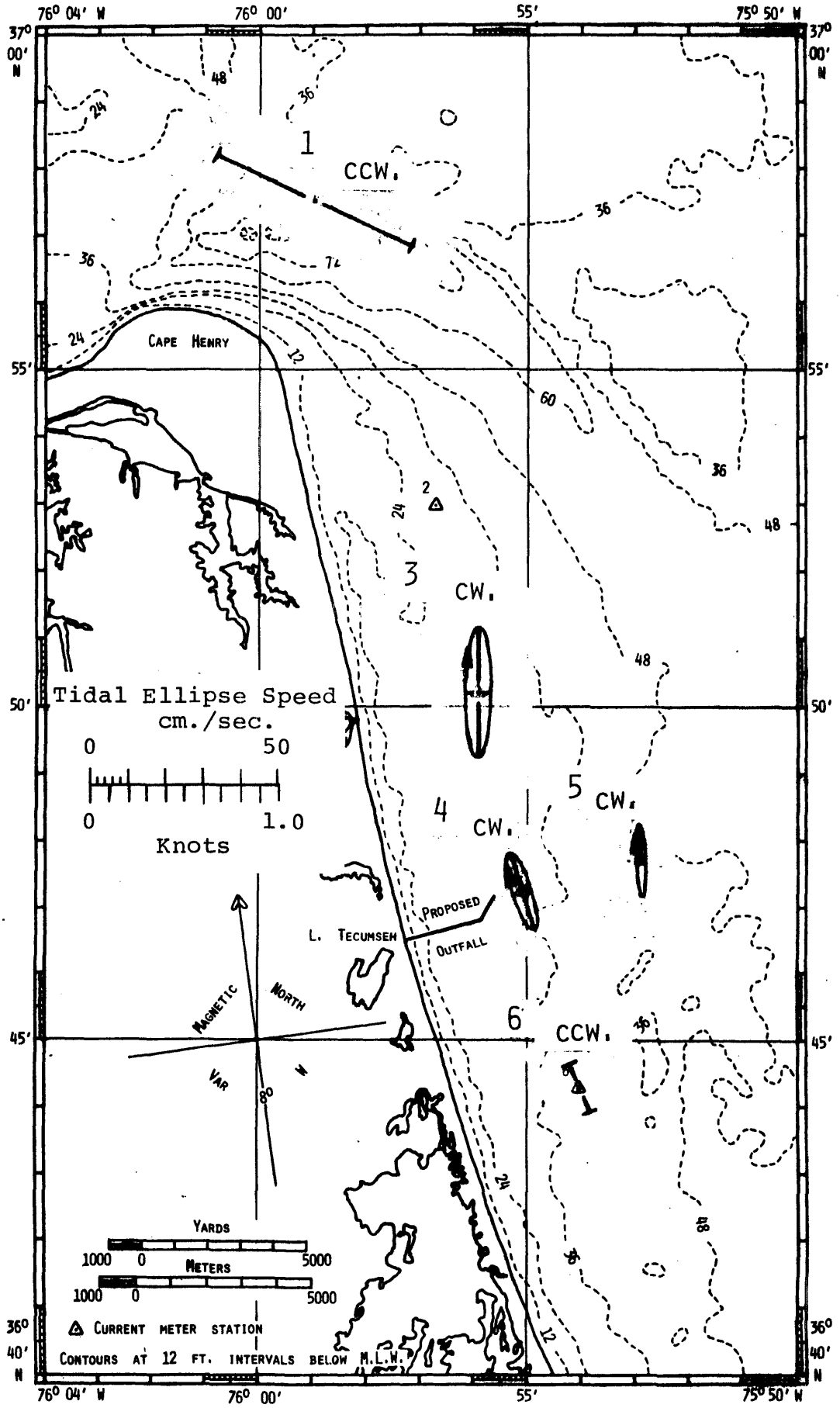

Figure 5.2b. Bottom current meter station M_2 tidal ellipses for Task I (stations 1, 3, 4, and 5) and Task III (station 6).

fluctuation. These long term variations are observable in the records, particularly those for task III after the calculated tide is subtracted from the records. They are more apparent in the surface than the bottom records, but they can be detected in the bottom records. These flow patterns are correlated, in this instance, with the meteorological onset of winter conditions (see section 5.8) and the passage of tropical storm Gilda towards the end of task III.

5.4.1 One way of representing these long term fluctuations is with amplitude spectra, produced as part of the TIPORAL program. These are similar to variance spectra, except that the square root of variance, or amplitude, is the ordinate rather than variance itself. Two such spectra are shown as figure 5.3 a,b. These are for the station of greatest interest, station 4 bottom, for tasks I and III. These figures show several features of interest which are common to all the records studied. The 29 day series length permits resolution of 5 tidal constituents, two diurnal and three semidiurnal, labelled O_1, K_1, N_2, M_2, and S_2 in the figures. The low frequency fluctuations mentioned above are seen as a rise in amplitude at the lowest frequencies calculated. In task III, the low frequency amplitudes approach 8 cm/sec., while in task I, they only approach about 2 cm/sec at low frequency.

5.4.2 The amplitude level at low frequency can be used to judge the representativeness of the mean value of current derived from the observed record. On the assumption that the level continues its trend towards low frequency, it follows that, were the record twice as long, a Fourier component would exist with

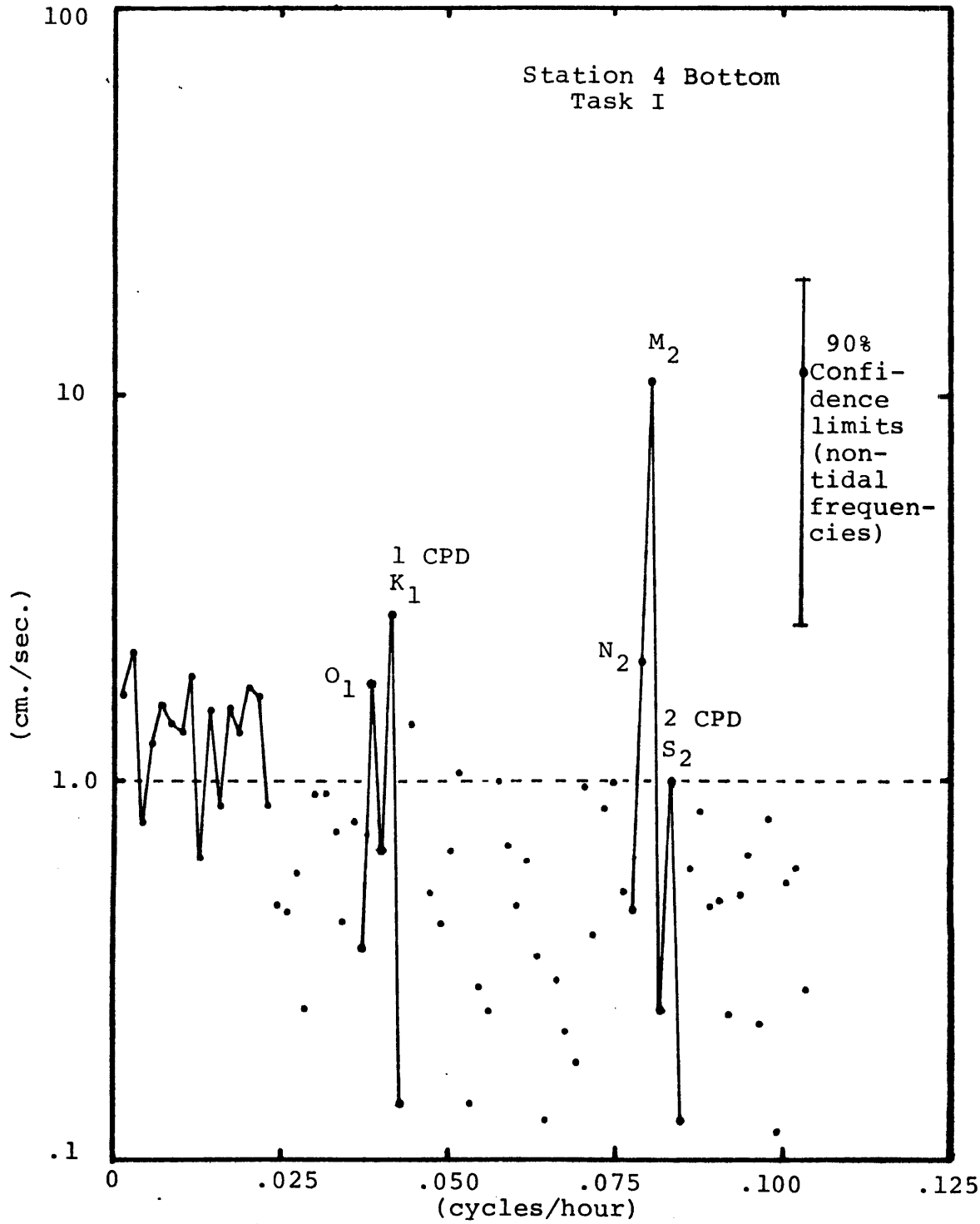

Figure 5.3a. Amplitude spectrum of coast parallel component of current for station 4, bottom, task I, Dam Neck, Virginia.

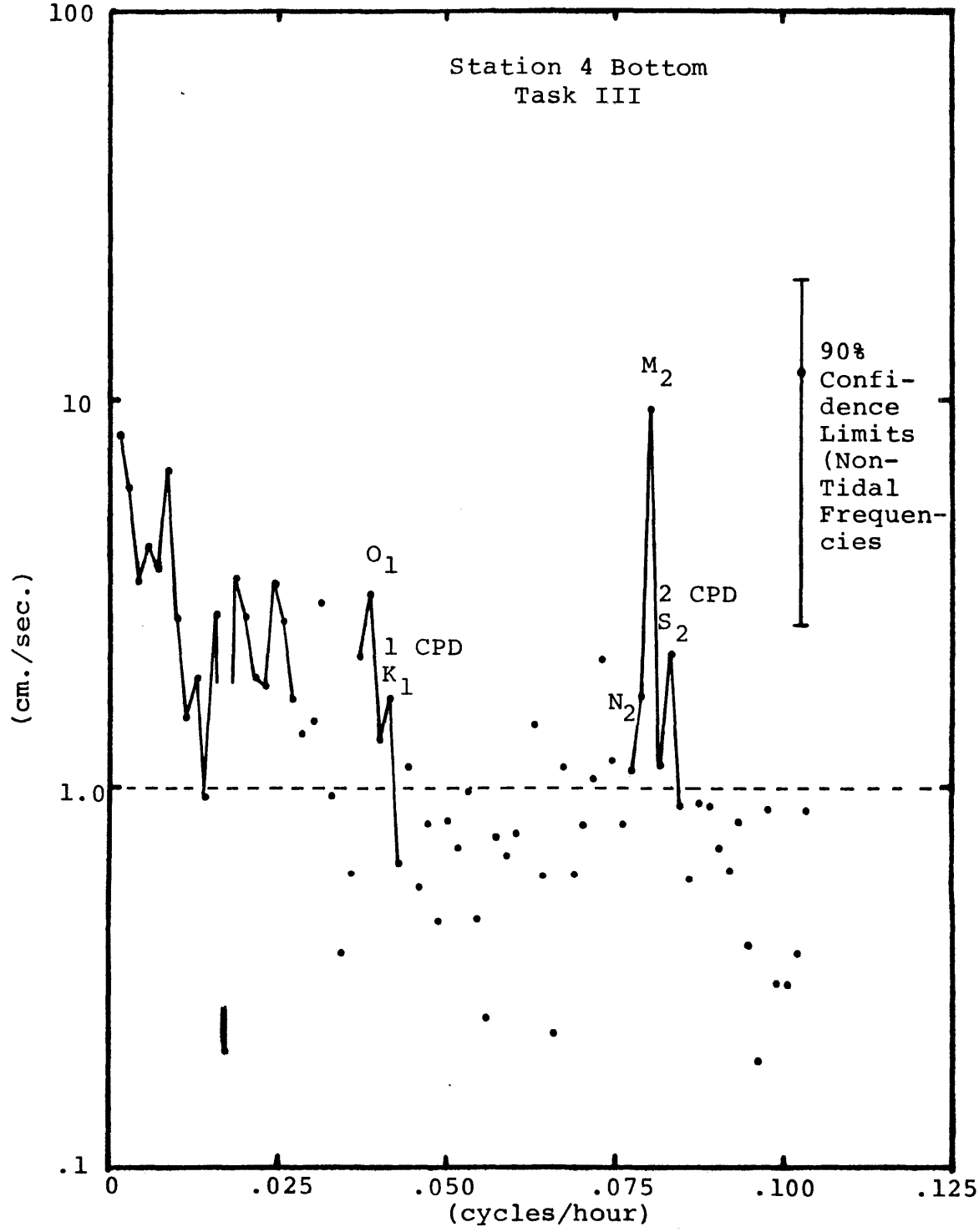

Figure 5.3b. Amplitude spectrum of coast parallel component of current for station 4, bottom, task III, Dam Neck, Virginia.

the amplitude of the low frequency value. This component, sampled for only half of its period, would produce an expected mean value over the 29 day series of about .41 times this amplitude level (see appendix 3). This value is .7 cm/sec for task I and 3.2 cm/sec for task III. The mean values calculated for these records are both close to these values, so they are not significantly different from zero. A similar comparison shows the mean values calculated at site 1 to be significantly different from zero.

5.4.3 Examination of the amplitudes for tidal currents at the five tidal constituent frequencies gives further insight into the data. The N_2 constituent has an amplitude of .192 $\pm$ .005 times the M_2 constituent in both records. This is precisely the ratio of the corresponding terms of the harmonic analysis of the tidal potential function. In contrast, the S_2 component with a period of exactly 12 hours has a different amplitude during each task, both of which are much less than the .465 times the M_2 given by the gravitational potential. Anomalous values for the S_2 tides are frequently encountered in tidal analysis (Wunsch, 1972) and can be related to a radiational tide and daily seabreeze affects. With this rationale, the change in the amplitude of the S_2 component between task I and task III can be attributed to a reduction of the seabreeze later in the year. The TIPORAL program assumes the S_2 tide to have its full gravitational potential value, so the anomalous value coupled with its expected strength leads to substantial

errors in the TIPORAL prediction. The O_1 and K_1 constituents are lower, with respect to the M_2, than the gravitational potential would suggest. This observation, equivalent to noting that the tide on the East Coast is of semi-diurnal type, is attributed to an oceanic resonance (Wunsch, 1972) near the M_2 frequency. For the purpose of prediction, the diurnal tides are not stable partly because another component (P_1) interferes with K_1 at the resolution of these spectra and partly because the general amplitude of all fluctuations approaches that of the diurnal components during Task III.

5.4.4 The level of the two spectra at periods of 2-5 days shows a slight indication of an additional broad peak. This may be the response associated with the passage of weather systems off Dam Neck.

5.5 The slack water time differences (predicted-observed) were calculated and plotted for several records (Figures 5.4 - 5.11). The average time difference for each record is given in Table 5.3 and indicated on the figures. Positive time differences correspond to slack water occurring at the current meter station before predicted slack water at Chesapeake Bay Entrance. Missing points arise when the longitudinal observed current did not reverse during a given tidal period.

The individual time differences are variable over the period of a month with approximately a 90 minute standard deviation. The mean values, shown by straight lines on the

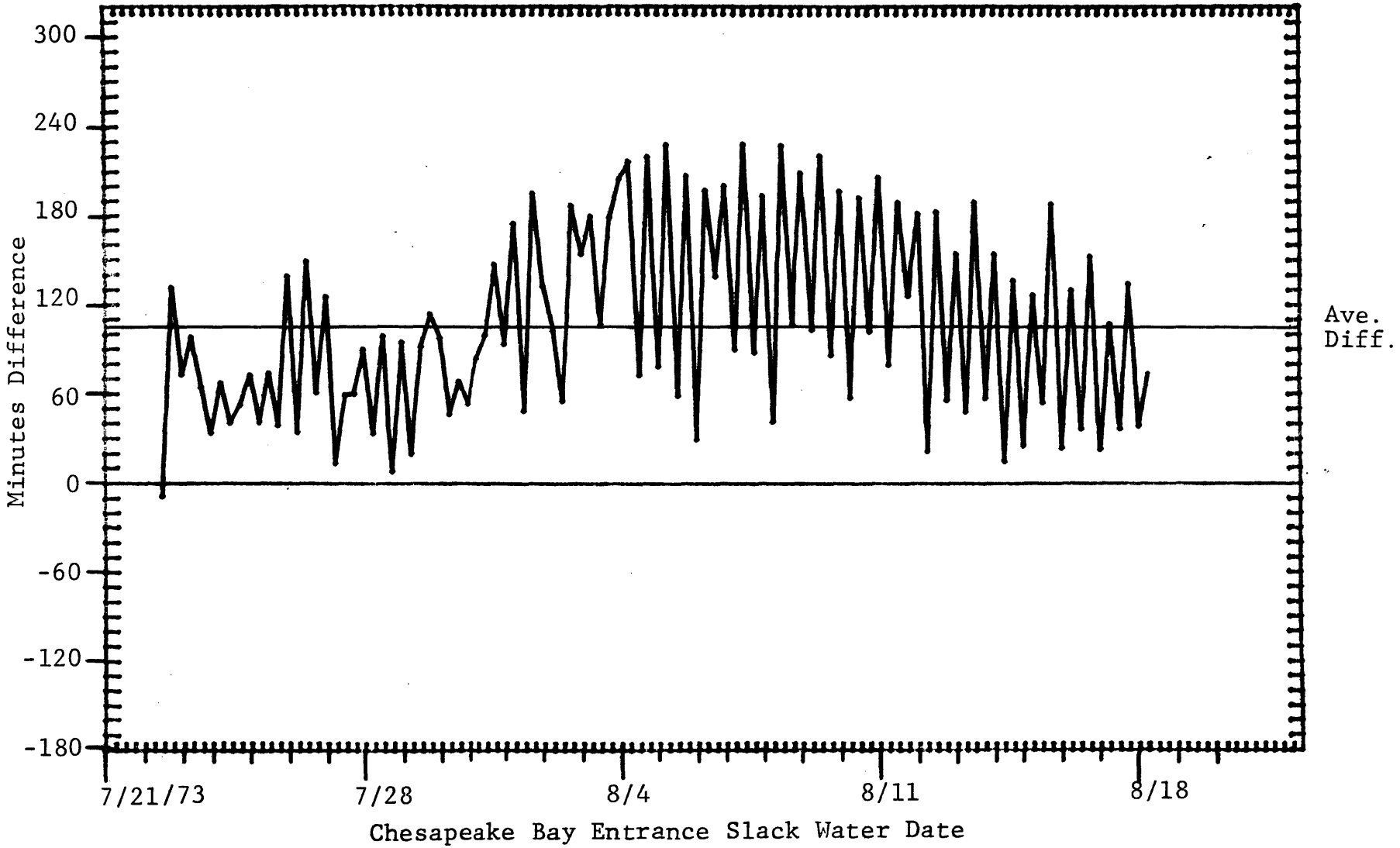

Figure 5.4. Slack water time difference: Time of predicted slack water at Chesapeake Bay Entrance minus time of observed slack water at Station 1, Surface, Task I.

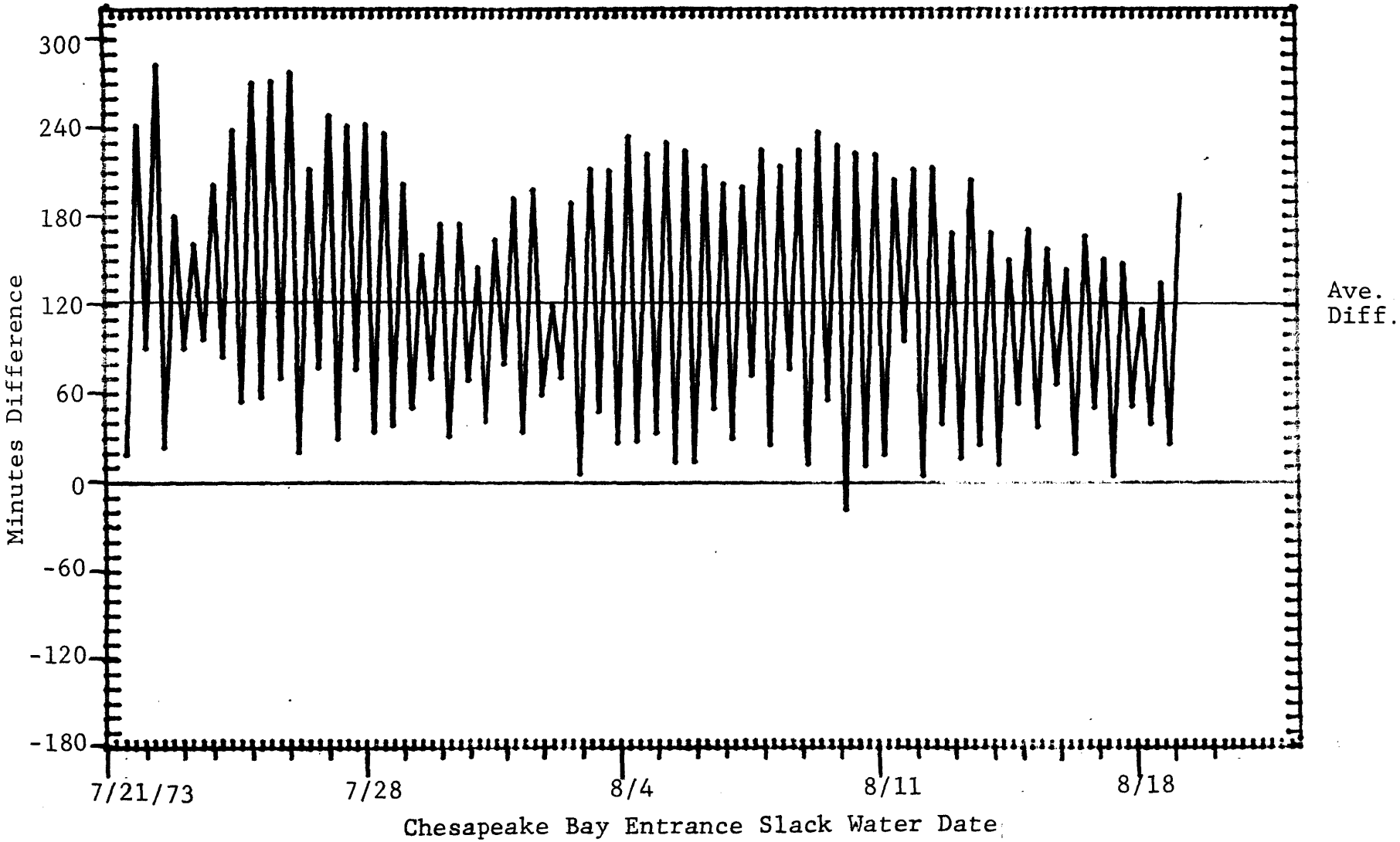

Figure 5.5. Slack water time difference: Time of predicted slack water at Chesapeake Bay Entrance minus time of observed slack water at Station 1, Bottom, Task I.

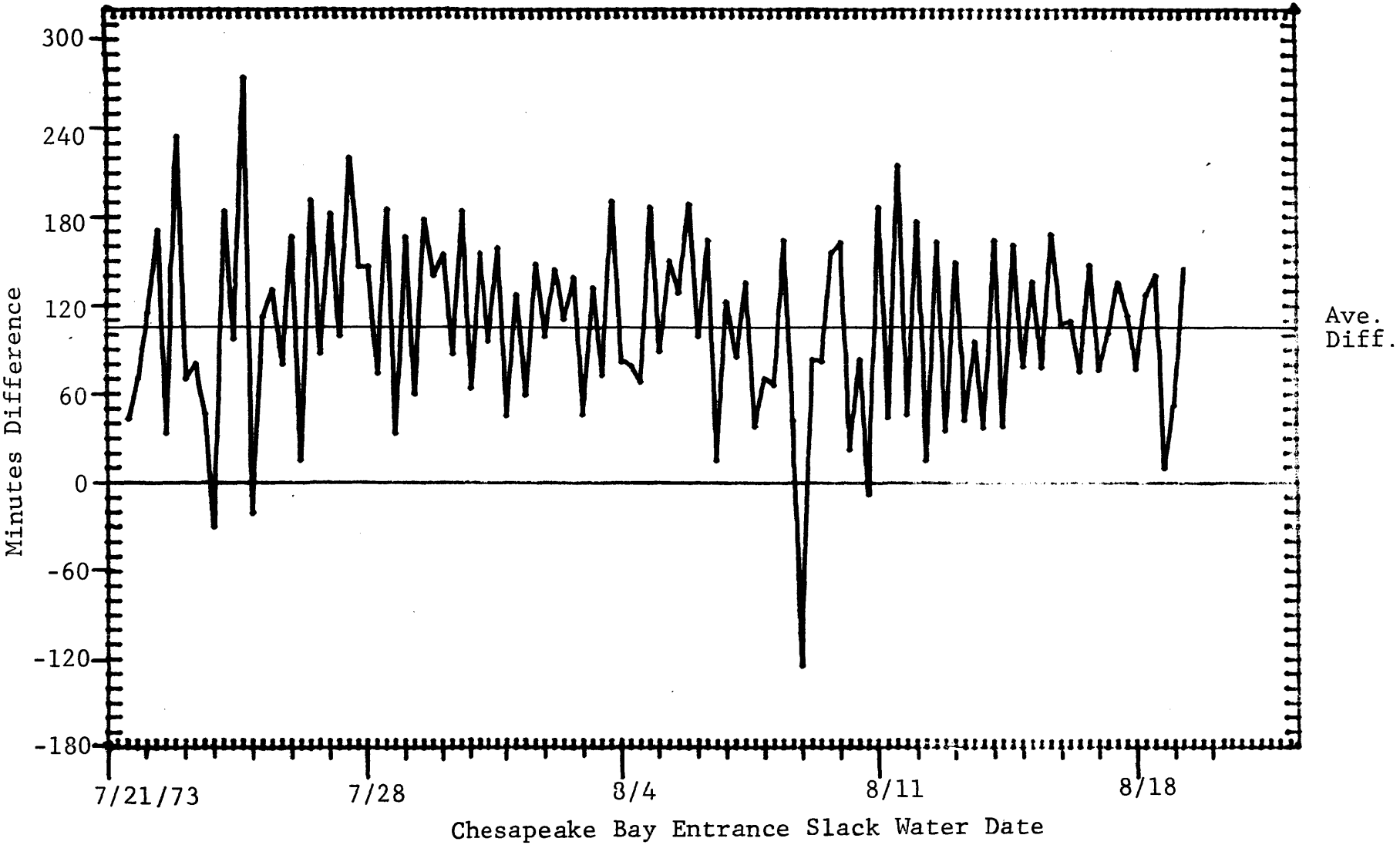

Figure 5.6. Slack water time difference: Time of predicted slack water at Chesapeake Bay Entrance minus time of observed slack water at Station 3, Bottom, Task I.

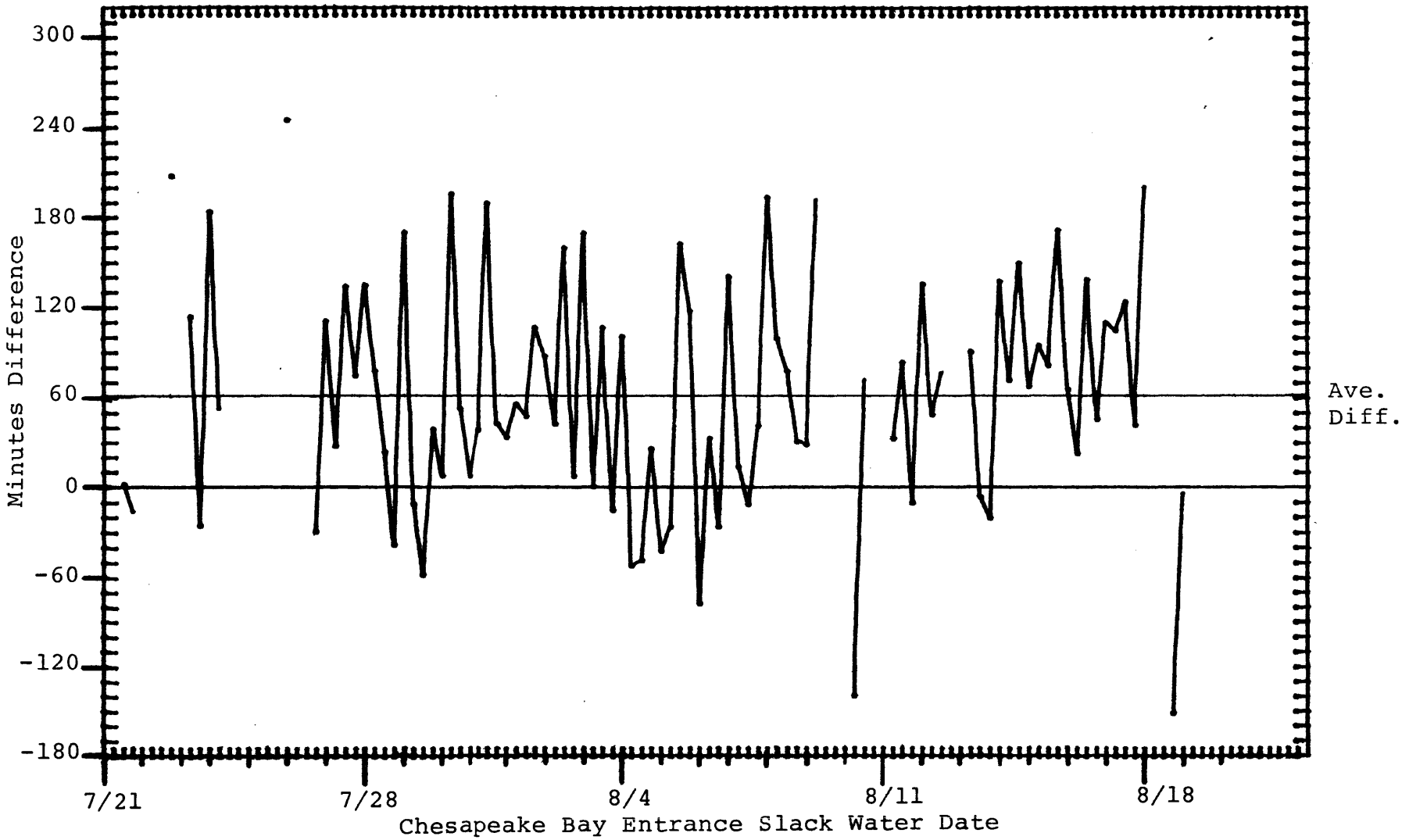

Figure 5.7. Slack water time difference: Time of predicted slack water at Chesapeake Bay Entrance minus time of observed slack water at Station 4, Surface, Task I.

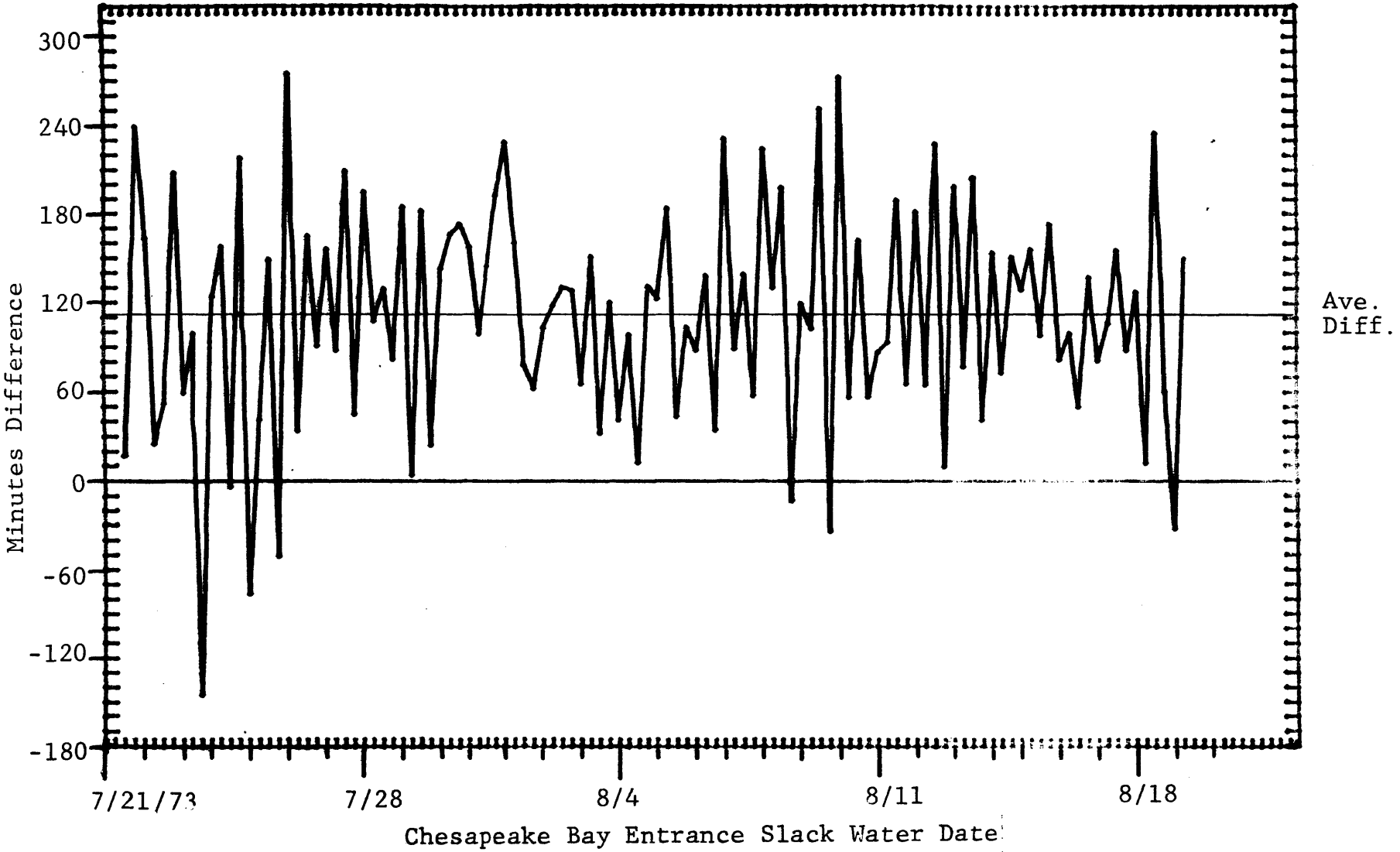

Figure 5.8. Slack water time difference: Time of predicted slack water at Chesapeake Bay Entrance minus time of observed slack water at Station 4, Bottom, Task I.

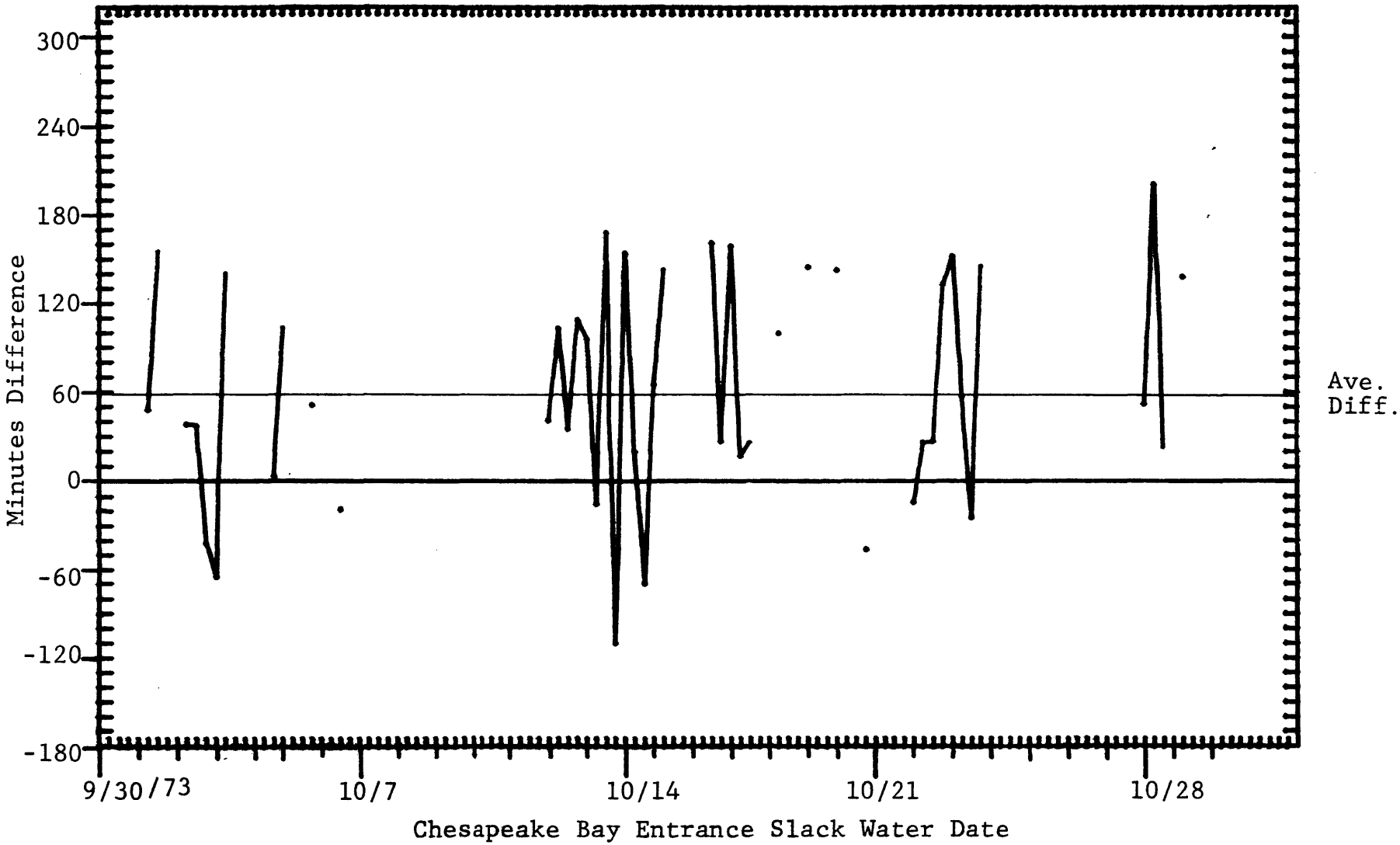

Figure 5.9. Slack water time difference: Time of predicted slack water at Chesapeake Bay Entrance minus time of observed slack water at Station 4, Surface, Task III.

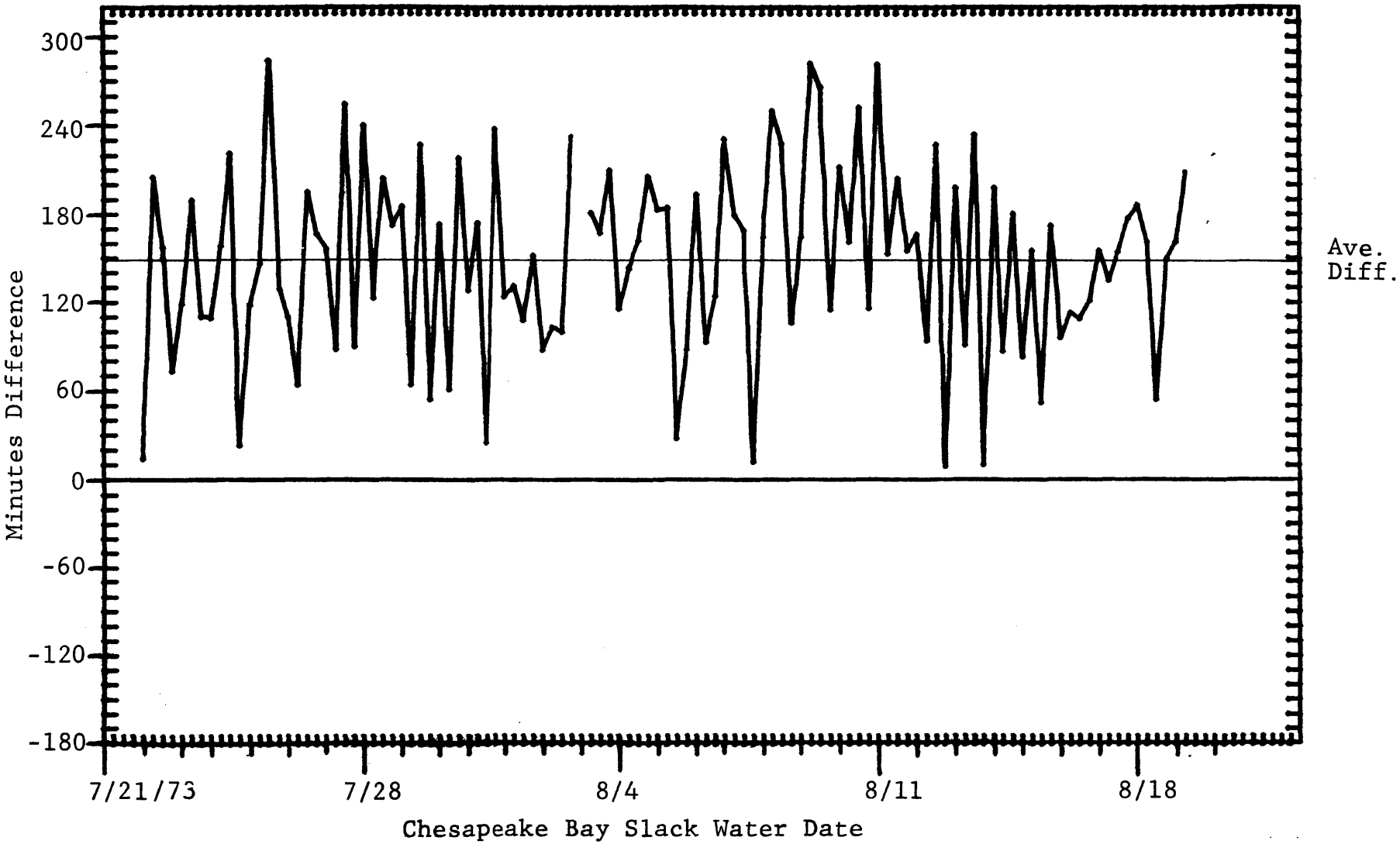

Figure 5.10. Slack water time difference: Time of predicted slack water at Chesapeake Bay Entrance minus time of observed slack water at Station 5, Bottom, Task I.

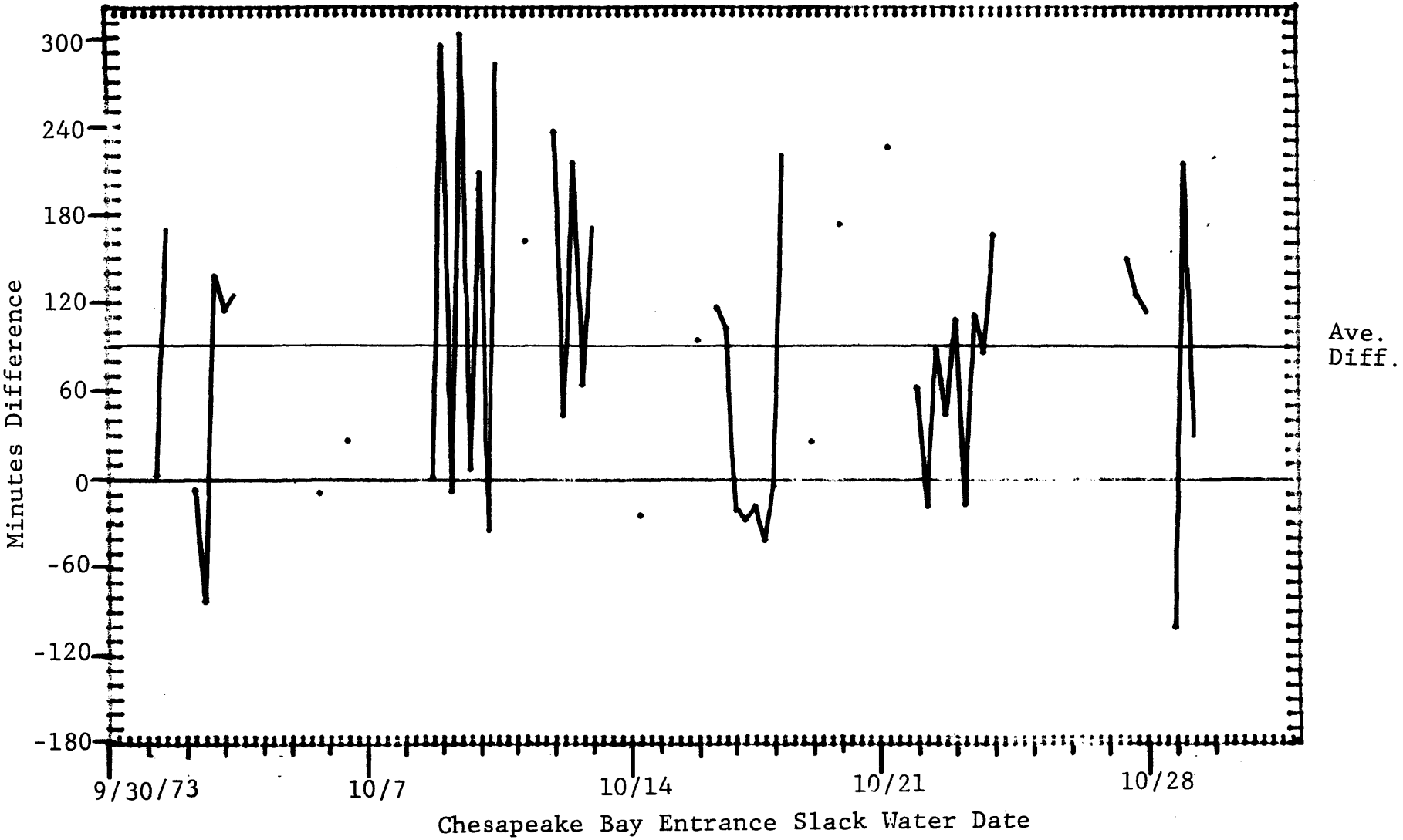

Figure 5.11. Slack water time difference: Time of predicted slack water at Chesapeake Bay Entrance minus time of observed slack water at Station 6, Bottom, Task III.

plots, appear to cluster around 60 minutes and 120 minutes. This may indicate an error in the time base of the records, but the time base data are not available to us for error tracing.

In view of the large variance in the graphs and the remaining uncertainties under any consistent set of assumptions regarding time base errors, we choose to draw no interpretations regarding the time difference between tidal heights and currents from these data. If a future experiment is attempted for this purpose, it should include current meters and tide guages, and the time basis should be identical to within at the most, 5 minutes.

5.6 The estimate of winter storm effects in the area is based on a different set of observations, those of drogued buoys tracked during the VIMS-NASA Langley Research Center joint EOLE program (Ruzecki, et al., 1976). A set of such tracks which passed through the study area during a winter storm is shown in figure 5.12. A feature of these tracks is a southerly drift associated with a winter storm. During this single event the four buoys involved experienced 50-80% of their total southerly excursion. The same data are shown in component (north and south) form in figure 5.13a,b. These are compared to the hypothesis that the current drift of the buoys (drogued at 2m depth) was 10% of the local wind velocity (Ruzecki, et al., 1976). The wind record shows the passage of two winter storms with wind speeds of up to 15 meters/second. These storms are during the times when the north displacement of the hypothesized wind drift decreases rapidly

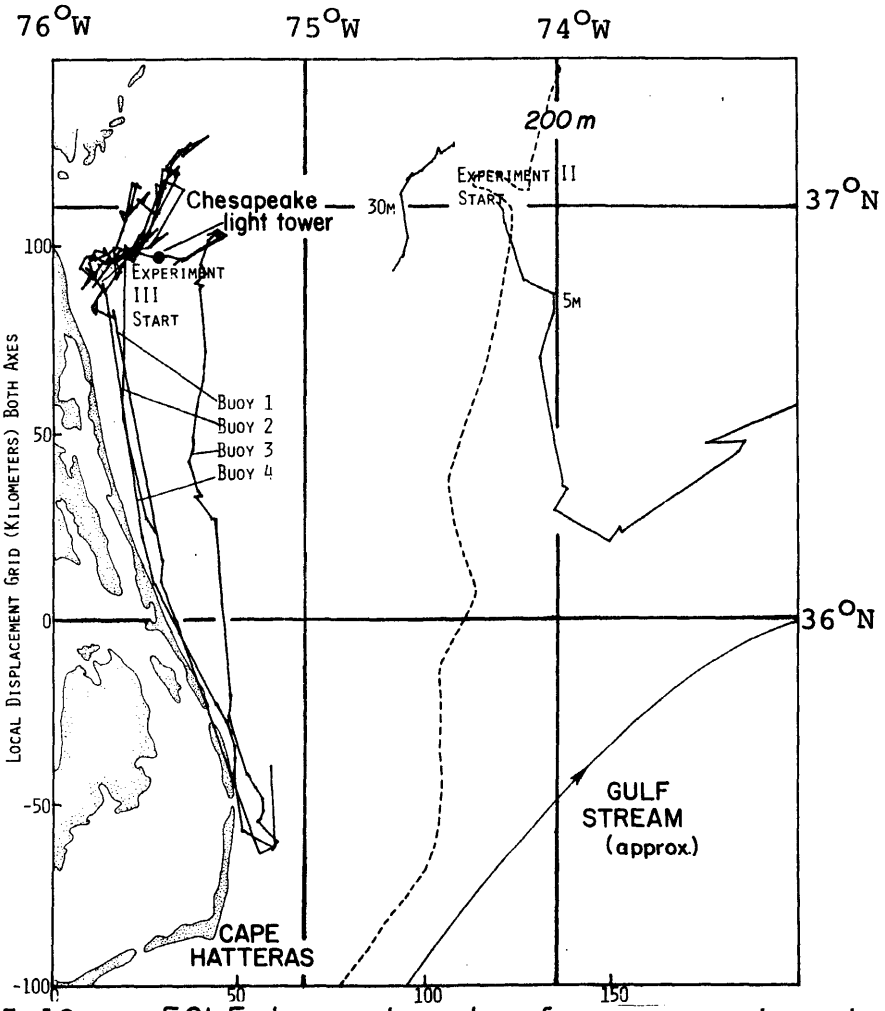

Fig. 5.12. - EOLE buoy tracks from experiments two and three, autumn, 1972.

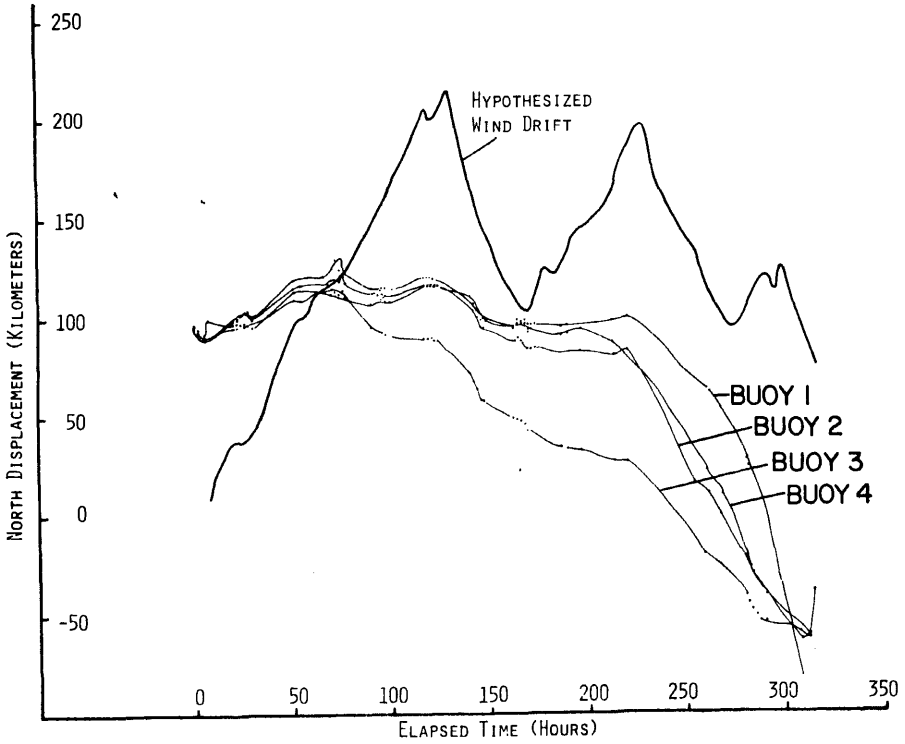

Fig. 5.13. - (a) North displacement of EOLE buoy tracks from experiment three compared to hypothesized wind drift.

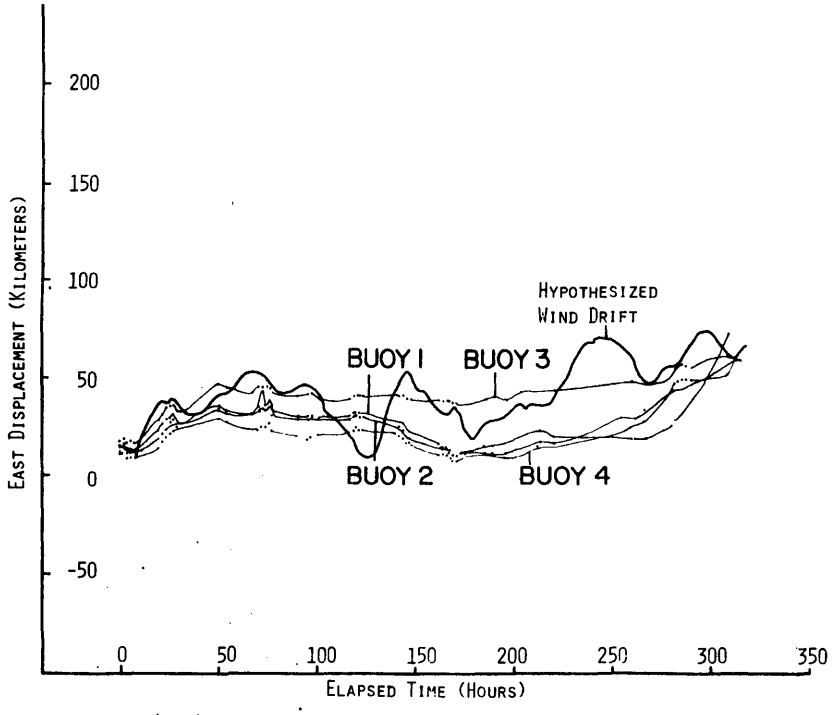

Fig. 5.13.- (b) East displacement of EOLE buoy tracks from experiment three compared to hypothesized wind drift.

with time. Notable is that the southerly buoy displacement is much greater during the second wind event than during the first one, the maximum speed being about 2 knots for a buoy travelling quite close to shore. It is this event which has led us to our estimate of winter storm currents.

5.6.1 The differences in displacement for similar local wind histories is a feature of the local shelf circulation. (Beardsley and Butman, 1974). It may be associated with the pattern of storm stress across the entire Middle Atlantic Bight, so that the local wind gives only part of the picture. When the strong southerly displacements occur, they are coherent across most of the width and length of the Mid-Atlantic Bight (Boicourt, 1976). A jet-like nearshore current has been attributed (ibid) to an additional current component from the mouth of Chesapeake Bay.

5.7 Hurricane Current Estimate

The local record of measured currents includes some passages of tropical disturbances. For example, tropical storm Gilda passed through while the EG&G current meter array was deployed for task III. These seem to indicate that currents caused by hurricanes are not likely to be much greater than those encountered during winter storms. Before accepting this conclusion, however, it may be that the particular way in which a hurricane approaches the coast can have a determining role in the maximum speeds which are attained. So we include an example from the Gulf Coast of a current meter set outside

the beach zone at a distance of 280 km (170 miles) from the landfall of hurricane Camille, August, 1969 (Murray, 1970). Recorded by this instrument were currents of 80 cm/sec (1.6 knots) with pulses to 160 cm/second (3.1 knots). The record was terminated five hours before the landfall of Camille by damage to the speed sensor. The direction sensor continued to function until two hours after landfall, at which time the signal connector was unplugged. This strong current was in the offshore direction. This single observation is not enough to make a prediction about currents to be expected in hurricanes at Dam Neck, but it is sufficient to note that the currents may be very strong compared to winter storm currents.

Another indication of the strength of hurricanes was reported by J. L. Krieg (1966) at the Hurricane Symposium of the American Society for Oceanography. In discussing pipelines for offshore oil and gas transport, he wrote,

"When is a pipeline likely to move? A pipeline is likely to move when it lies on the bottom in water depths where either orbital wave particles or broad currents can act against a substantial length of the line. Most pipeline movement in the Gulf of Mexico has been restricted to small diameter lines because the larger diameter lines have been buried."
Such movement, as Krieg reported, has occurred in water deeper than one hundred feet.

Hurricanes and tropical storms are not frequent phenomena in the local area, but it is likely that an offshore outfall will

have to withstand several during its lifetime. For cataloguing purposes, the U. S. weather bureau classifies a hurricane as a storm with winds in excess of 74 mph (64 knots) and a tropical storm as a storm with winds above 39 mph (34 knots) and below hurricane speeds. With this convention, Cry (1965) reported 2 hurricanes crossing the shoreline of Virginia, Maryland, Delaware or New Jersey between 1901 and 1963. For the same time period and coastline section, one tropical storm crossed the shore, 10 hurricanes and 45 tropical storms passed within 300 miles of the coast, the region in which coastal influence is generally experienced. We can summarize these data by establishing an experience rate .89 hurricanes or tropical storms having any effect on the Dam Neck region in a given year.

5.8 Winter Storm Occurrence

5.8.1 Winter storms or "northeasters" are a regular feature of the winter season in the mid-Atlantic Bight. They are low pressure features which typically first form over the Gulf Coast states and pass across the coast between Cape Hatteras and Cape Henry. While not all of them do this, after passing offshore, they typically intensify while continuing their tracks in a north-easterly direction until they are well past the Gulf of Maine. The nearshore passage of one of these storms is marked by heavy precipitation and winds from the northeast followed by a frontal passage, clearing, colder, and initially strong winds from the north veering towards west.

5.8.2 These storms seem intimately related to a regularly occurring frontal region, the Polar front. This feature recedes towards the north during summer and advances southwards in the winter. In the eastern U.S., it appears as a cold front crossing Virginia in a south-east direction. It is plausible that the onset of the winter storm season corresponds to the first crossing of the local coast by this front in the autumn. At least, in the set of weather charts examined from the VIMS collection, no winter storms occurred before this time of year, about September 15. The front crosses and recrosses the local area during the winter season, the crossings being frequently associated with storms. The final recession in a given season, about April 15, occurs when the summer high pressure area, the Bermuda High, first reaches a central pressure of 1028 mb.

6. References

Beardsley, Robert and Bradford Butman, "Circulation on the New England Continental Shelf - Response to Strong Winter Storms", Geophysical Research Letters 1 (4), August 1974.

Boicourt, W. C. and P. W. Hacker, "Circulation on the Atlantic Continental Shelf of the United States, Cape May to Cape Hatteras, Memoires Societi Royale des Sciences de Luge, (6), X, 1976.

Cry, George W., "Tropical Cyclones of the North Atlantic Ocean" Tracks and Frequencies of Hurricanes and Tropical Storms, 1871-1963", Technical Paper No. 55, Laboratory of Climatology, U. S. Weather Bureau, Washington, D. C. (1965).

E.G.&G. Environmental Engineering Services, (1973), unbound and untitled current meter logs, E.G.&G. Environmental Engineering Services, Waltham, Mass.

Goldsmith, Sutton and Sallenger (1973), "Bathymetry of the Virginian Sea", Virginia Institute of Marine Science, Gloucester Pt., Va.

Krieg, Joe L., "Hurricane Risks as they Relate to Offshore Pipelines," in Hurricane Symposium, American Society for Oceanography Publication Number One, October 1966.

Lewis, James K., "The Analysis of Short Term Tidal Data," unpublished M.S. thesis, College of William and Mary, 1975, 105 pp.

Ludwick, John C. and William J. Saumsiegle, "Sediment Stability at the Dam Neck Disposal Site, Virginia", Old Dominion University Institute of Oceanography, Technical Report No. 27, January, 1976.

Magas, A., 1973, "Oceanographic Report - Virginia Beach Outfall Study, Virginia Beach, Va.", E.G.&G. Environmental Engineering Services, Waltham, Mass.

Malcolm Pirnie Engineers, Inc., "Engineering Report, Advanced Wastewater Treatment, Atlantic Wastewater Treatment Plant, Virginia Beach, Virginia, June 1974 revised December, 1974.

Malcolm Pirnie Engineers, Inc., 1976a, "Relation Between Bottom Profile Locations by Ocean Systems, Inc., and Geotechnical Engineering Co.". (unbound drawing).

Malcolm Pirnie Engineers, Inc., 1976b, "Atlantic Plant Outfall - Phase I". (unbound blueprint).

Malcolm Pirnie Engineers, Inc., 1976c, "Atlantic Plant Outfall - Phase II". (unbound blueprint).

Munk, W. H., and D. E. Cartwright, "Tidal Spectroscopy and Prediction", Phil. Trans. Roy. Soc., A., 259, pp. 533-581, 1966.

Murray, Stephen P., "Bottom Currents near the Coast during Hurricane Camille", Journal of Geophysical Research, 75 (24), August 20, 1970.

National Ocean Survey, Tidal Current Tables, 1973, Atlantic Coast of North America, 1972.

National Ocean Survey, 1974, C&GS 1227, "Cape Henry to Currituck Beach Light", 11th Ed., Mar. 16/74.

National Ocean Survey, 1975, NOS 12221, "Chesapeake Bay Entrance", 39th Ed., Mar. 22/75.

Ruzecki, E. P., Christopher Welch, Jim Usry, and John Wallace, "The Use of the EOLE Satellite System to Observe Continental Shelf Circulation", Proceedings of the Offshore Technology Conference, May 1976.

Saumsiegle, W. J., "Stability and Local Effects of an Offshore Sand Storage Mound, Dam Neck Disposal Site, Virginia Inner Continental Shelf", M.S. Thesis, Old Dominion University, Norfolk, Va., 1976.

Schureman, Paul, Tide and Current Glossary, National Ocean Survey, Washington, D. C. 1975.

U. S. Department of the Interior, Geological Survey, 1965, "Virginia Beach Quadrangle, Virginia, Virginia Beach City, 7.5 Minute Series (Topographic) 1965. (photo-revised 1970).

Usry, J. W. and J. W. Wallace, "Data Report of Six Free-Drifting Buoys Tracked by the EOLE Satellite in the Western North Atlantic Ocean in the Autumn of 1972", NASA Technical Memorandum X-72645, February, 1975.

Wallace, John W. and John W. Cox, "Design, Fabrication and Systems Integration of a Satellite Tracked, Free-Drifting Ocean Data Buoy," NASA Technical Memorandum X-72817, January, 1976.

Wallace, John W. and J. W. Usry, "Data Report of Four Free-Drifting Buoys Tracked by the EOLE Satellite in the Western North Atlantic Ocean in the Winter of 1973," NASA Technical Memorandum X-72768, September, 1975.

Wunsch, Carl I., "Bermuda Sea Level in Relation to Tides, Weather, and Baroclinic Fluctuations", Reviews of Geophysics 10, (1), February 1972.

APPENDIX 1. Chart of Dam Neck Area

A1.1 Summary - This appendix includes discussions and descriptions of the following aspects of Figure A1.1:

a) Source Data

b) Construction Technique

c) Errors

A1.2 Source Data

a) Shoreline and interior

1) The Cape Henry to Currituck Beach Light Chart (C&GS 1227) includes the shoreline and interior of the Virginia Beach area as well as lines of latitude and longitude.

b) Current meter station locations:

1) Current meter logs (E.G.& G. 1973) contain the latitude and longitude of each current meter station to the nearest 0.1 minute. The logs are unbound and untitled and are not part of E.G. & G.'s formal report.

2) The oceanographic report prepared by E.G. & G. (Magas, 1973) has two charts showing the plotted locations of the current meter stations. The report deals exclusively with current meter deployment and results. E.G. & G. submitted it to Hydroscience, and Hydroscience forwarded it to Malcolm Pirnie.

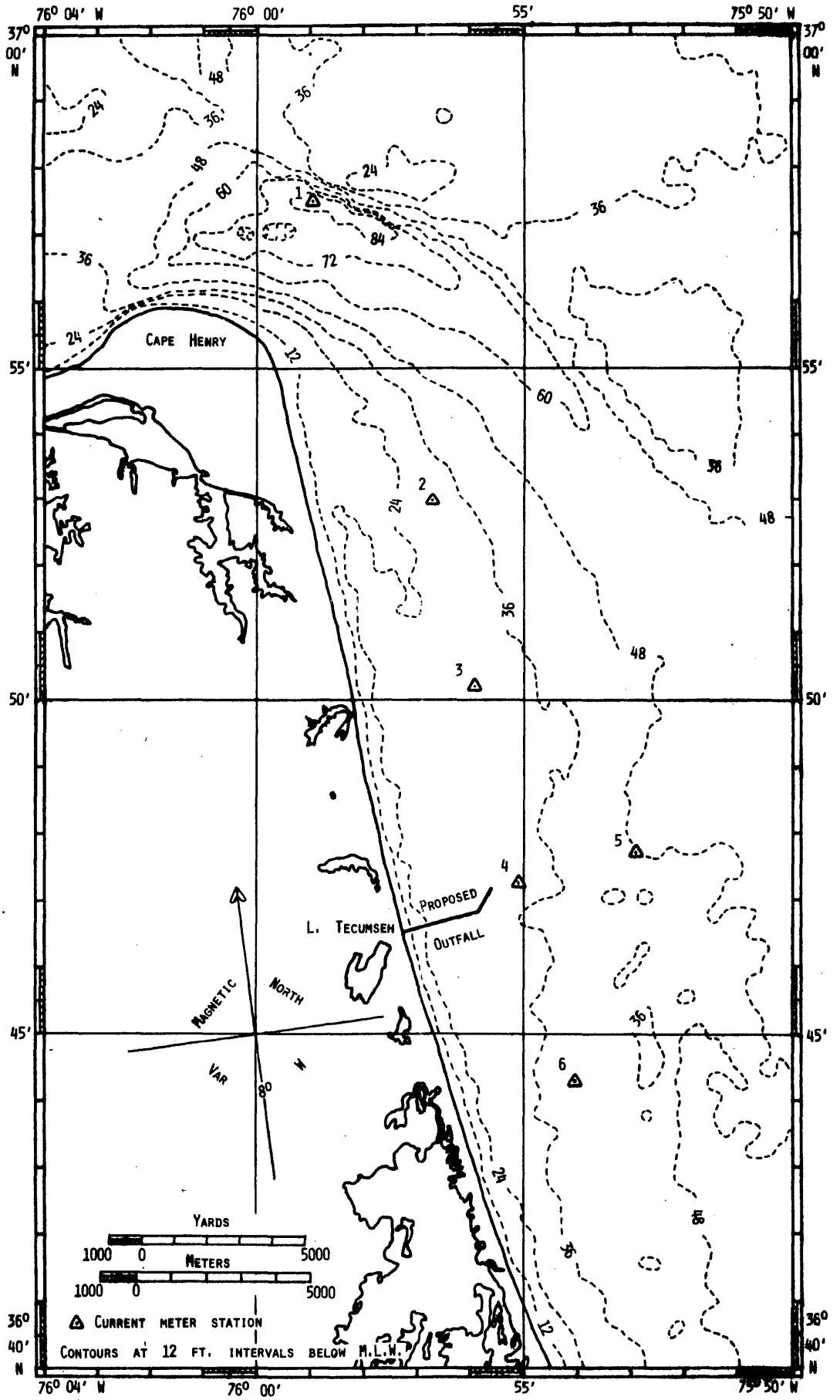

Figure A1.1. Location of proposed outfall at Dam Neck, Virginia. Current meter stations are included along with bathymetry (Goldsmith, Sutton and Sallenger, 1973 and Ludwick and Saumsiegle, 1976).

c) Location of proposed outfall:

1) The engineering report prepared by Malcolm Pirnie (Malcolm Pirnie, 1974) gives the orientation of the outfall and diffuser sections.

2) The three drawings by Malcolm Pirnie (Malcolm Pirnie, 1976a, 1976b, and 1976c) give the dimensions of the outfall and diffuser sections. The third drawing (1976c) is the most detailed and useful.

d) Depth contours:

1) The chart prepared by Goldsmith, et al. (Goldsmith, et al., 1973) has depth contours at 6 ft. intervals below mean low water (MLW). These are based on depths taken from the original Hydrographic Sounding Sheets (boat sheets) of the area. The chart includes the Virginia Beach area east of $76^{o}1.5'$ W and south of $37^{o}00'$ N.

2) The Chesapeake Bay Entrance chart (NOS 12221) has individual depth values west of $76^{o}1.5'$ W.

3) The thesis written by W. J. Sausiegle (Ludwick and Saumsiegler, 1976) has depth contours of the offshore sand storage mound located about 6 km east of Rudee Inlet. The bathymetry of the sand storage mound is not included in recent NOS charts or in Goldsmith, et al. (1973).

A1.3 Figure Construction Technique

a) Figure A1.1 was constructed primarily by tracing the source data:

1) The shoreline, interior, and lines of latitude and longitude were traced from C&GS 1227.

2) The current meter stations were traced from Magas (1973).

3) The depth contours were traced from Goldsmith et al. (1973) using a Map-O-Graph for reduction.

b) The outfall and diffuser sections were drawn on a topographic map of the area (U. S. Dept. of Interior, 1963). This drawing was photoreduced and transferred onto the original of Figure A1.1.

c) Figure A1.1 is 50% photoreduction of the original drawing.

A1.4 Errors

a) The errors associated with Figure A1.1 are given in Table A1.1.

b) The plotted current meter station locations were compared with their recorded positions given on the current meter logs. The positions all coincided within 90 m (the accuracy of the recorded positions) except as noted below:

1) Station 4, Surface, Task I (4 Surf. I) and Station 4 Bottom, Task I (4 Bot. I). The recorded position was the same as 3 Surf. I. We presumed this was an error.

Table A1.1. Errors in Figure A1.1

Item	Error	Cause
Shoreline, interior, lines of latitude and longitude	30 meters (m)	alignment and tracing problems
Current meter station locations (See A1.4(b))	80 m.	alignment and tracing problems plus a distortion between the charts in Magas (1973) and Figure A1.1.
Proposed outfall and diffuser sections	60 m. length 0.25° orientation	alignment and tracing problems
Depth contours	200 m in position 1.5 m in depth	The position errors resulted from alignment and tracing problems plus distortions between the bathymetry chart and Figure A1.1 The depth error resulted from inherent errors in the soundings

2) 4 Surf. II and 4 Bot. II were not compared because we do not have copies of their film recording logs.

3) 1 Surf. III had a recorded position 360 m north of the recorded position of 1 Bot. III. Since each current meter mooring consisted of a surface and bottom current meter, we presume that one of these recorded positions is in error. The position of 1 Bot. III is within 90 m of the plotted position for station 1.

4) 4 Surf. III and 4 Bot. III had recorded positions 450 m south of their plotted positions.

We presume that the current meter stations given in the formal report (Magas, 1973) are correct.

APPENDIX 2. Current Meter Data Processing

A2.1 Summary - This appendix covers the following topics:

a) The original Dam Neck current meter data as received from Malcolm Pirnie Engineers, Inc. and Old Dominion University.

b) The Dam Neck current meter data after conversion to VIMS format.

c) TIPORAL program description and users guide.

A2.2 Original Dam Neck Current Meter Data

a) The current meters sampled at 5 minute intervals. EG&G reduced these data to 15 minute average readings and transferred the averaged readings to magnetic computer tape. Further information regarding sensitivity, deployment, and calibration may be found in Magas (1973).

b) The data are organized as follows:

1) File number - Each current meter record was individually numbered from 1 to 23. We received 23 files of data from Malcolm Pirnie Engineers, Inc. and one "file" of data from Old Dominion University (file 24).

2) Current meter record number - a 6 digit number identifying each current meter record.

3) Date and time of first current meter reading - listed in numerical month, day, hour, minute format.

4) Number of observations in data record.

5) Current meter station number.

6) Location of current meter - surface or bottom.

7) Task number.

8) Speed factor - a correction factor for the speed readings. Each listed speed reading must be multiplied by this factor to obtain the correct speed reading.

9) Current meter direction - three digit direction from 0-359 degrees. We assumed the direction was in degrees true.

10) Current speed - three digit speed, in whole mm/sec.

c) The data was checked for completeness and the results are given in Table 3.2.

1) The current meter for station 1, bottom, task III (1 Bot. III) produced no data.

2) Incorrect header labels - files 20 and 21 are incorrectly labeled station 6 surface task I. According to the E.G.&G. current meter logs, these files actually contain data for station 6 bottom task I.

3) Five minute current meter data - It appears that file 21 is a copy of the 5 minute interval current meter data for 6 Bot. I.

d) A computer listing of the original data is kept at VIMS.

e) E.G.&G. current meter logs and data plots.

1) The logs appear to be work sheets/records used during current meter data reductions. They include such pertinent information as current meter identification numbers, sampling scheme, location and depth, start and stop times, and comments on the overall quality of the data. The logs for 4 Surf. II and 4 Bot. II are missing.

2) The plots include a histogram of rotor speed, polar coordinate histogram plot of direction, and a plot of rotor speed versus direction.

3) A copy of the logs and plots is kept at VIMS.

A2.3 Dam Neck current meter data converted to VIMS format.

a) The current meter data was converted to the VIMS current meter data format (Table A2.1) to be compatible with VIMS software.

b) Header labels were added to each current meter file. Nominal depth was not included.

1) Latitude and longitude were obtained from a chart of the sampling area (Magas, 1973).

2) Depths of the current meters are in feet below mean low water.

3) File 20 and 21 were labeled task 1, station 6, bottom.

4) The file 21 current readings are considered to be at 5 minute intervals.

Table A2.1. VIMS Current Meter Data Format

1st record on the file contains:

Current Meter Type	A1
Section	A4
Station	A2
Nominal Depth	I4
Actual Depth (ft)	F10.3
Degrees of Longitude	A3
Minutes of Longitude	A2
Seconds of Longitude	A2
Degrees of Latitude	A3
Minutes of Latitude	A2
Seconds of Latitude	A2

2nd record on the file contains:

Starting Time:	Month (1-12)	I2
	Day (1-31)	I2
	Year	I4

and the remaining records each contain eight:

Time of Day (0000-2359)	I4
Speed (in fps)	F8.3
Direction (000-359 degrees magnetic)	I3

Note: "A" indicates alpha format.

"I" indicates integer format.

"F" indicates floating point format.

The logical record length is 120 bytes (one character per byte) and the block size is 3600 bytes.

5) Values of latitude, longitude and depth are given in Table 3.3.

c) Data Conversion Program - A data conversion program was written for a tape-to-tape conversion.

The reformatted header labels were inserted at the beginning of each file.

The conversion calculations were:

1) Speed

(mm/sec) x (0.00328084 ft/mm) x
(speed multiplier) = ft/sec.
rounded to nearest thousandth of a ft/sec.

2) Direction

degrees true + 8 degrees = degrees magnetic

NOTE: Bad readings, identified by a series of 9's in the original data were kept as 9's in the converted data.

3) Time of Day - Calculated from initial reading.

d) Current Meter Data Editing - The editing consisted of scanning the converted data for instances of two bad readings, which were discovered in only a single instance. Interpolated values were generated to replace these readings for station 6, surface, task I. This was necessary because the original data has two consecutive bad readings on July 24th at 0735 and 0750, and the analysis program interpolates for only one bad reading. The two interpolated readings comprise less than .1% of the 2780 readings for this station.

e) The edited data are stored on a computer tape labeled VCM 093 at the College of William and Mary Computer Center. A printout of these data is kept at VIMS.

A2.4 TIPORAL (Tidal Potential Ratio Lag) Program

a) The TIPORAL program (Lewis, 1975) was used to fourier analyze the current meter data and corresponding potential tide.

b) Program Output - The current meter readings are broken down into orthogonal components. In this case, we chose ~355°m to be the longitudinal (longshore) component and ~85°m to be the lateral (perpendicular to shore component). For each orthogonal component, the program lists:

1) Average current speed (cm/sec)
2) The first 72 fourier components, periods (hrs), amplitude (cm/sec), and phase (degrees) for:
   a) current meter data
   b) tidal potential data
3) Amplitude ratios and phase lags between the current meter data and the tidal potential data.
4) Precision of reproduction (a measure of how closely the tidal potential represents the actual current meter values).
5) Plot of current meter data for every current reading.

For the subsequent "manipulating" runs the program:

6) Plots the manipulated tidal potential values for the time and location of every current meter reading.

7) Plots the "residual current" values for the time and location of every current meter reading. These are the values of the difference between the actual current readings and the manipulated tidal potential.

c. TIPORAL Program Users Guide

1) The TIPORAL program is written in PL1. The program was modified to accept variable length current meter records. The modified program is entitled TIPREV1.

2) The program accesses and processes current meter data tapes as specified in the data control cards.

3) The computer processing consists of at least two computer runs as follows:

a) First run

1) Punch data control card including the maximum number of current meter readings to be processed. Format is I4 followed by a semi-colon";" e.g. (beginning in column 1) 2784;

2) Punch requested data station control cards as follows: DATE='MMDDYY', SECT='TSK- ',(1,2, or 3),STAT=' ',

(1,2,3,4,5,or 6),DPTH=' ',(two digit depth listed in Table 3.3),CHNOR= ; (longitudinal magnetic channel axis, 000-359). e.g. (beginning in column 1)

DATE='072173',SECT='TSK1',STAT='4', DPTH='26',CHNOR=355;

NOTE: Requested data cards must be organized in ascending date, section, station, depth, order.

3) Insert these cards just before the "//" card at the end of the computer cards.

4) Complete computer job request (run time ~40 min) and submit to computer center.

b) Manipulating runs

1) Read amplitude ratios and phase lags from computer listing.

2) Change the semi-colon on the data station cards to a comma.

3) Punch amplitude ratios and phase lag data control cards as follows:

a) Longitudinal components (beginning in column 1 where X's indicate the maximum allowable data size).

NDAMP=XXXXXXXXX,NDPHAS=XXX.XX,
NSAMP=XXXXXXXXX,NSPHAS=XXX.XX,
NQAMP=XXXXXXXXX,NQPHAS=XXX.XX,

In the variables, N stands for longitudinal, AMP - amplitude ratio, PHAS - phase lag, D - diurnal, S - semidiurnal, Q - quarterdiurnal.

b) Lateral components are punched similarly except the variables are headed by an "E" instead of "N".

c) An example of the data control input for a manipulating run follows:

```
DATE='072173',SECT='TSK1',
STAT='4',DPTH='26',CHNOR=355,
NDAMP=57904,NDPHAS=126.32,
NSAMP=704302,NSPHAS-106.24,
NQAMP=0,NQPHAS=0,EDAMP=4794,
EDPHAS=277.45,ESAMP=92875,ESPHAS=
-67.45,EQAMP=0,EQPHAS=0;
```

d) Remove the first run data station control cards and insert these cards just before the "//" end card.

e) Submit the job as before.

f) A copy of the TIPREV program is kept at VIMS.

A2.5 Processed Data - Current meter data for the following stations were processed by the TIPREV1 program: station 1 surface task I (1 Surf. I), 1 Bot. I, 1 Bot. III, 3 Bot. I, 4 Surf. I, 4 Bot. I,4 Bot. II, 4 Surf. III, 4 Bot. III, 5 Bot. I, 6 Bot. III. Both Fourier analysis and potential tide manipulations were performed for all these stations (except 6 Bot. III, for which no tidal manipulations were performed). Computer printouts of these results are stored at VIMS.

APPENDIX 3. Mean Value Significance Evaluation

If a cosine wave is sampled randomly over half of its period, what is the expected value of the absolute value of the mean value of the resulting curve? If we call this I, it can be expressed as:

$$I = \left\langle \left| \frac{2}{T} \int_{a}^{a+T/2} \cos \frac{2\pi t}{T} \, dt \right| \right\rangle$$

where a can be uniformly located between 0 and T.

The inner integral evaluates to a single sine function, so we can replace the expected value symbols with an average and a straightforward calculation.

$$I = \frac{1}{T} \int_{o}^{T} \frac{2}{\pi} \left| \sin \frac{2\pi a}{T} \right| da$$

The absolute value of a sine curve repeats the first half cycle over the second half, and so

$$I = \frac{4}{\pi T} \int_{o}^{T/2} \sin \frac{2\pi a}{T} \, da = \frac{4}{\pi 2}$$

So $I = .405$

If a trend in an amplitude spectrum towards low frequency exhibits a level L for the amplitude of the lowest frequency fluctuation, the expected value of the mean calculated from this data is .405L on the assumption of zero long term mean and a continuation of the trend to half the lowest resolvable frequency.